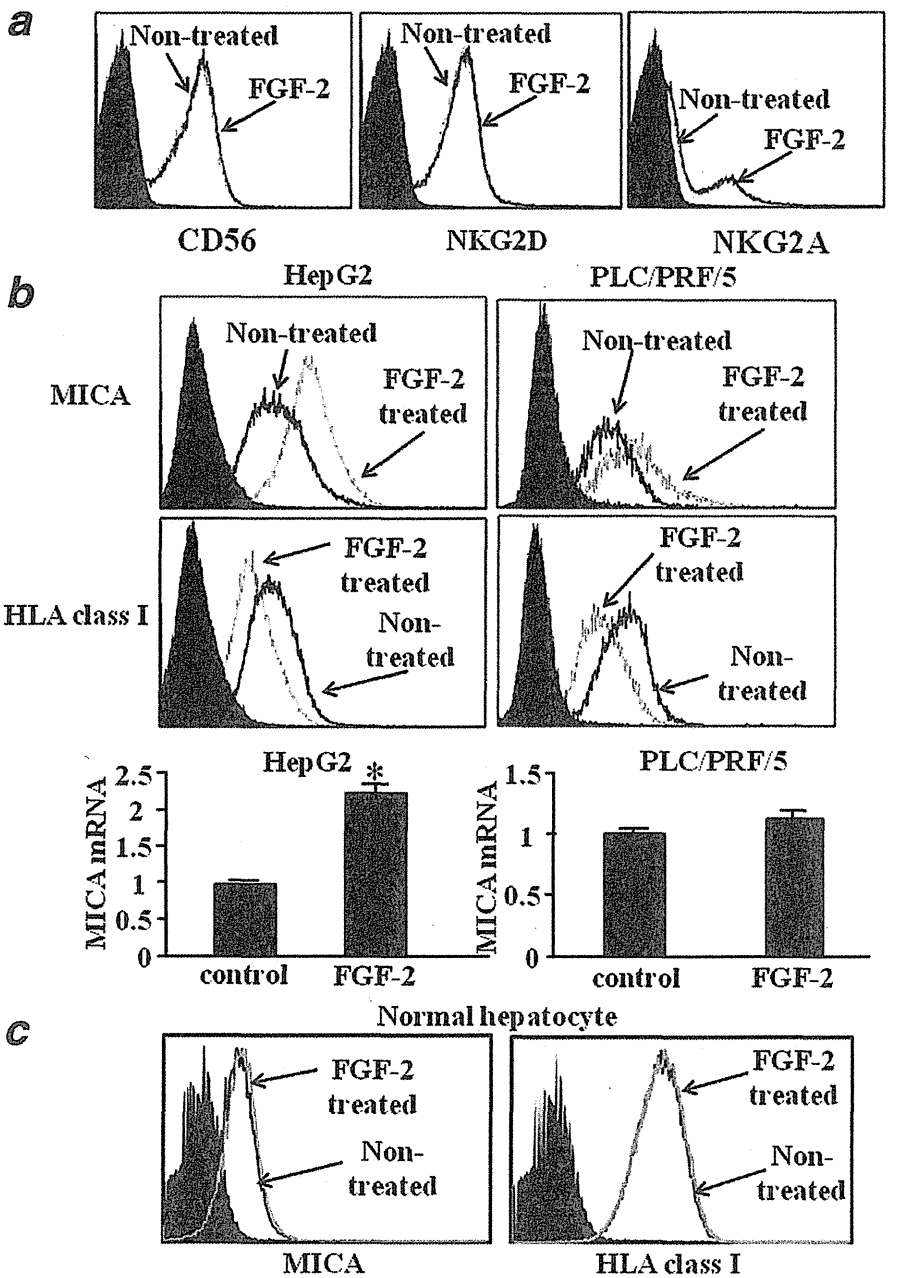

Figure 3. The expressions of NKG2D and NKG2A on FGF-2-treated NK cells and the expressions of MICA and HLA class I on FGF-2-treated hepatoma cells. (*a*) The expressions of NKG2D or NKG2A on FGF-2-treated or nontreated NK cells were evaluated. NK cells obtained from healthy volunteers (2×10^6 cells/well) were cultured with or without FGF-2 protein (250 ng/ml) for 24 hr, and the expressions of NKG2D and NKG2A on NK cells were evaluated by flow cytometry. Representative results were shown. (*b,c*) HCC cells (B: HepG2 and PLC/PRF/5) or normal hepatocytes (*c*) were treated with 250 ng/ml FGF-2 or control medium for 48 hr and subjected to flow cytometric analysis of MICA and HLA class I surface expression. Black line histograms: MICA or HLA class I staining of nontreated cells; gray line histograms: MICA or HLA class I staining of FGF-2-treated cells; shaded/black histograms: control IgG isotype Ab staining of each molecule. (*b*) *Lower panel*, mRNA levels of MICA in FGF-2-treated or nontreated HCC cells were examined by real-time PCR. Representative data are shown. Similar results were obtained from two independent experiments. * $p < 0.05$.

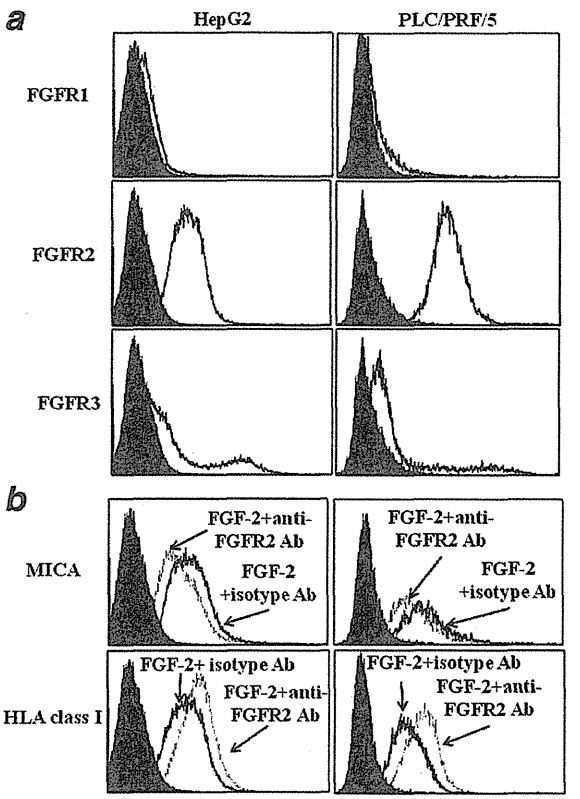

Figure 4. The expressions of FGF receptors on hepatoma cells. (*a*) The expressions of FGF receptors (FGFR1, FGFR2, and FGFR3) on both HepG2 and PLC/PRF/5 cells were evaluated by flow cytometry. Black line histograms: staining of each FGF receptors (FGFR1, FGFR2, FGFR3), shaded/black histograms: control isotype Ab staining of each molecule. (*b*) To confirm that adding of FGF-2 protein resulted in modifying the expressions of MICA and HLA class I on both HCC cells, the expressions of both molecules on FGF-2- (250 ng/ml) treated HCC cells with anti-FGFR2 neutralizing Ab (10 μg/ml) or isotype control Ab (murine isotype control IgG 10 μg/ml) were evaluated by flow cytometry. FGF-2+anti-FGFR2 Ab, the expression of MICA or HLA class I on FGF-2-treated HCC cells with anti-FGFR2 neutralizing Ab. FGF-2+isotype Ab, the expression of MICA or HLA class I on FGF-2-treated HCC cells with isotype control Ab. shaded/black histograms: control isotype Ab staining of each molecule. Representative results were shown. Similar results were obtained in three independent experiments.

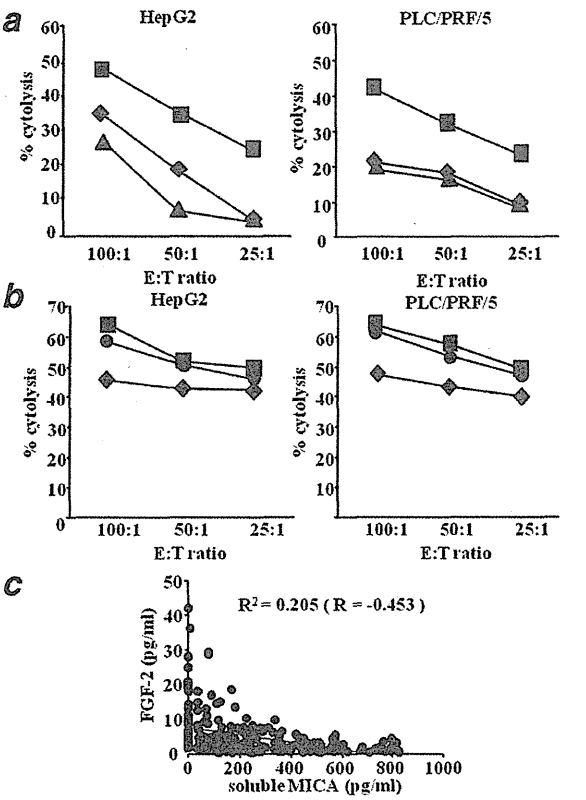

Figure 5. The cytolytic activity against FGF-2-treated HCC cells and the correlation between serum FGF-2 and soluble MICA in patients with chronic liver disease. (*a,b*) Both HepG2 and PLC/PRF/5 cells were cultured with or without FGF-2 protein (250 ng/ml) for 48 hr, and the cytolytic activities of NK cells against FGF-2-treated HepG2 and PLC/PRF/5 cells or nontreated HCC cells were evaluated by ^{51}Cr-release assay. Nontreated HCC cells (◆) or FGF-2-treated HCC cells without (■) or with blocking Ab of MICA/B (6D4) (*a*, ▲) or isotype IgG Ab (*b*, ●). Representative results are shown. Similar results were obtained from three independent experiments. (*c*) Correlation of serum FGF-2 levels and soluble MICA levels in patients with chronic liver disease (chronic hepatitis patients, N = 80, liver cirrhosis patients, N = 84 and HCC patients, N = 112). The serum FGF-2 and soluble MICA were evaluated by specific ELISA respectively.

increased expression of membrane-bound MICA. We next examined the correlation of serum FGF-2 and soluble MICA in patients with chronic liver disease. Serum FGF-2 levels in patients with chronic liver disease correlated with soluble MICA levels (Fig. 5c). These results suggested that high FGF-2 levels in patients with chronic liver disease may prevent the shedding of MICA in liver tissues.

Discussion

The FGF-2 levels in chronic liver disease, a premalignant condition, have not been well studied. Uematsu *et al.* reported that the serum FGF-2 levels of patients with LC or HCC were significantly higher than those of HVs, and serum FGF-2 levels of HCC patients tended to be lower than those of LC patients without HCC.[6] In contrast, Jinno *et al.* reported that the circulating FGF-2 levels in HCC patients were significantly higher than those in CH and LC patients.[16] In the present study, we analyzed the serum FGF-2 levels on

a larger scale for patients with chronic liver disease. Consistent with Uematsu's report, the serum FGF-2 levels significantly decreased along the progression of chronic liver disease and those in HCC patients were significantly lower than those in CH or LC patients. These results suggested that decreasing FGF-2 levels might be associated with the occurrence of HCC during the progression of chronic liver disease. FGF-2 has been shown to act as a potent angiogenic factor in a number of cell lines and solid tumors.[1,2] As for HCC development, FGF-2 has been reported to augment vascular endothelial growth factor (VEGF)-mediated angiogenesis in HCC development.[17] However, at present, in contrast to the clear roles of VEGF in the angiogenesis of HCC, the roles of FGF-2 in the HCC development are still controversial and should be elucidated.

Immunohistochemical analysis revealed that hepatocytes in patients with chronic liver diseases seemed to produce FGF-2, but those in healthy donors did not. This suggested that inflammatory responses in liver tissues might have roles in the production of FGF-2. Some inflammatory cytokines, such as IL-1β and IL-6, increased in CH or LC patients.[13–15] Aside from liver cells, IL-6 could induce FGF-2 expressions in basal cell carcinoma cell line[18] or Kaposi's sarcoma cell and human umbilical vein endothelial cells.[19] On the basis of these reports, we examined the effect of such inflammatory cytokines on FGF-2 expression in HCC cells and normal hepatocytes. The FGF-2 expression could be, at least in part, induced by IL-1β and IL-6. Both IL-1β and IL-6 are produced mainly by local immune cells, including activated Kupffer cells.[20] Although the detail mechanism of the induction of FGF-2 expression in HCC cells and normal hepatocytes is little known, the production of these cytokines might contribute to preventing HCC development *via* promoting FGF-2 expression in the liver.

Guerra *et al.* reported that NKG2D-deficient mice are defective in tumor surveillance in models of spontaneous malignancy,[11] suggesting that NK-dependent immune-surveillance might play a critical role in tumor development. However, the mechanism of tumor surveillance of NK cells remains unclear in HCC development. We previously demonstrated that membrane-bound MICA on HCC cells plays essential roles in the NK sensitivity of HCC cells.[21] We therefore evaluated the MICA (activating molecule of NK cells) and HLA class I (inhibitory molecule of NK cells) on HCC cells treated with FGF-2. This treatment resulted in increasing MICA expression and decreasing HLA class I on HCC cells. Consistent with these results, the cytolytic activity of NK cells against FGF-2-treated HCC cells was higher than that against nontreated HCC cells. These results suggested that FGF-2 enhanced the NK sensitivity of HCC cells by upregulating MICA expression and downregulating HLA class I on the cellular surface. Interestingly, adding FGF-2 did not change the expressions of MICA and HLA class I on normal hepatocytes. These demonstrated that FGF-2 could enhance the NK sensitivity of HCC cells but not that of normal hepatocytes. We also evaluated the expressions of MICA and HLA class I on other growth factors (such as VEGF or PDGF)-treated HCC cells. The expressions of MICA and HLA class I on VEGF- or PDGF-treated HCC cells were similar to those on nontreated HCC cells (Tsunematsu H, unpublished data). In this study, we demonstrated that FGF-2 production from liver tissues decreased along the progression of chronic liver disease. FGF-2 production from liver tissues might prevent the occurrence of HCC by eliminating HCC cell by enhancing NK sensitivity. If the innate immunity of the liver can be efficiently activated, preventing the occurrence of HCC could be expected. We previously demonstrated that anti-HCC chemotherapy and molecular targeted therapy using sorafenib resulted in enhancing NK sensitivity of HCC cells *via* upregulation of membrane-bound MICA on HCC cells.[12,22] These results suggested the possibility of new routes for chemoprevention of HCC, which could improve the prognosis of chronic liver disease patients. Also, on the basis of our results, FGF-2 supplementation therapy may be a rational approach for eliminating HCC cells in the chronic liver disease.

The concentration of FGF-2 in our *in vitro* study was high compared with the serum FGF-2 concentration level. Previous reports demonstrated that FGF-2 produced in the liver tissues acts in an autocrine or paracrine fashion.[2,5] We demonstrated that serum FGF-2 levels in chronic liver disease were significantly higher than those in HVs and that serum FGF-2 levels decrease with the progression of liver disease. These results suggested that FGF-2 production from liver tissues might also decrease with the progression of liver disease. Although the local FGF-2 concentration in the liver tissues still remains unknown and may differ from the serum FGF-2 concentration, our results have at least demonstrated that FGF-2 could enhance NK sensitivity of HCC cells *via* modification of the activating and inhibitory molecules on HCC cells.

The expression of NKG2D has been reported in all NK cells. However, this has also been reported in most NKT cells, subsets of γδ T cells and all human CD8+ T cells and a subset of CD4+ T cells.[23] In addition to NK cells, the MICA-NKG2D pathway plays roles in the costimulation or recognition of each cell. Our results demonstrated that FGF-2 might increase the membrane-bound MICA on HCC cells. It might be possible that the increased expression of MICA may also activate other lymphocytes expressing NKG2D and that these cells may also contribute to the elimination of HCC cells.

The earlier results suggested that FGF-2 levels might contribute to the eradication of HCC cells in liver tissues, which would prevent the incidence of HCC in chronic liver disease. Our patients' data demonstrated that HCC occurrence of the patients with high levels of FGF-2 was significantly lower than that with low levels of FGF-2, which is consistent with the results of NK sensitivity of FGF-2-treated HCC cells. Moreover, the FGF-2 levels in patients before HCC occurrence were significantly higher than those in the same

patients after HCC occurrence. The decreasing levels of serum FGF-2 may be a prediction factor for the occurrence of HCC in chronic liver disease.

Despite recent progress in understanding HCC development, unknown mechanisms remain. We have shown here that FGF-2 levels in chronic liver disease were significantly higher than those in HVs, and serum FGF-2 levels decreases along the progression of liver disease. Importantly, FGF-2 enhances NK sensitivity of HCC cells *via* modification of the activating and inhibitory molecules on HCC cells. These findings suggested that FGF-2 might play roles in eliminating occurring HCC cells by innate immunity.

References

1. Pang R, Poon RT. Angiogenesis and antiangiogenic therapy in hepatocellular carcinoma. *Cancer Lett* 2006;242:151–67.
2. Mise M, Arii S, Higashituji H, Furutani M, Niwano M, Harada T, Ishigami S, Toda Y, Nakayama H, Fukumoto M, Fujita J, Imamura M. Clinical significance of vascular endothelial growth factor and basic fibroblast growth factor gene expression in liver tumor. *Hepatology* 1996; 23:455–64.
3. Chow NH, Cheng KS, Lin PW, Chan SH, Su WC, Sun YN, Lin XZ. Expression of fibroblast growth factor-1 and fibroblast growth factor-2 in normal liver and hepatocellular carcinoma. *Dig Dis Sci* 1998; 43:2261–6.
4. El-Assal ON, Yamanoi A, Ono T, Kohno H, Nagasue N. The clinicopathological significance of heparanase and basic fibroblast growth factor expressions in hepatocellular carcinoma. *Clin Cancer Res* 2001;7:1299–305.
5. Kin M, Sata M, Ueno T, Torimura T, Inuzuka S, Tsuji R, Sujaku K, Sakamoto M, Sugawara H, Tamaki S, Tanikawa K. Basic fibroblast growth factor regulates proliferation and motility of human hepatoma cells by an autocrine mechanism. *J Hepatol* 1997;27:677–87.
6. Uematsu S, Higashi T, Nouso K, Kariyama K, Nakamura S, Suzuki M, Nakatsukasa H, Kobayashi Y, Hanafusa T, Tsuji T, Shiratori Y. Altered expression of vascular endothelial growth factor, fibroblast growth factor-2 and endostatin in patients with hepatocellular carcinoma. *J Gastroenterol Hepatol* 2005;20:583–8.
7. Fattovich G, Stroffolini T, Zagni I, Donato F. Hepatocellular carcinoma in cirrhosis: incidence and trends. *Gastroenterology* 2004;127:S35–50.
8. Bosch FX, Ribes J, Diaz M, Cleries R. Primary liver cancer: worldwide incidence and trends. *Gastroenterology* 2004;127: S5–16.
9. Doherty DG, O'Farrelly C. Innate and adaptive lymphoid cells in human liver. *Immunol Rev* 2000;174:5–20.
10. Mehal WZ, Azzaroli F, Crispe IN. Immunology of the healthy liver: old questions and new insights. *Gatsroenterology* 2001;120:250–60.
11. Guerra N, Tan YX, Joncker NT, Choy A, Gallardo F, Xiong N, Knoblaugh S, Cado D, Greenberg NM, Raulet DH. NKG2D-deficient mice are defective in tumor surveillance in models of spontaneous malignancy. *Immunity* 2008;28:571–80.
12. Kohga K, Takehara T, Tatsumi T, Miyagi T, Ishida H, Ohkawa K, Kanto T, Hiramatsu N, Hayashi N. Anti-cancer chemotherapy inhibits MICA ectodomain shedding by downregulating ADAM10 expression in hepatocellular carcinoma. *Cancer Res* 2009;69:8050–7.
13. Lapinski TW. The levels of IL-1β, IL-4 and IL-6 in the serum and the liver tissue of chronic HCV-infected patients. *Arch Immunol Ther Exp* 2001;49: 311–16.
14. Bortolami M, Kotsafti A, Cardin R, Farinati F. Fas/FasL system, IL-1β expression and apoptosis in chronic HBV and HCV liver disease. *J Viral Hepat* 2008; 15:515–22.
15. Migita K, Abiru S, Maeda Y, Daikoku M, Ohata K, Nakamura M, Komori A, Yano K, Yatsuhashi H, Eguchi K, Ishibashi H. Serum levels of interleukin-6 and its soluble receptors in patients with hepatitis C virus infection. *Human Immunol* 2005; 67:27–32.
16. Jinno K, Tanimizu M, Hyodo I, Kurimoto F, Yamashita T. Plasma level of basic fibroblast growth factor increases with progression of chronic liver disease. *J Gastroenterol* 1997;32:119–21.
17. Yoshiji H, Kuriyama S, Yoshii J, Ikenaka Y, Noguchi R, Hicklin DJ, Huber J, Nakatani T, Tsujinoue H, Yanase K, Imazu H, Fukui H. Synergistic effects of basic fibroblast growth factor and vascular endotherial growth factor in murine hepatocellular carcinoma. *Hepatology* 2002; 35:834–42.
18. Jee SH, Chu CY, Chiu HC, Huang YL, Tsai WL, Liao YH, Kuo ML. Interleukin-6 induced basic fibroblast growth factor-dependent angiogenesis in basal cell carcinoma cell line via JAK/STAT3 and PI3-kinase/Akt pathways. *J Invest Dermatol* 2004;123:1169–75.
19. Faris M, Ensoli B, Kokot N, Nel AE. Inflammatory cytokines induce the expression of basic fibroblast growth factor (bFGF) isoforms required for the growth of Kaposi's sarcoma and endothelial cells through the activation of AP-1 response elements in the bFGF promoter. *AIDS* 1998;12:19–27.
20. Oyanagi Y, Takahashi T, Matsui S, Takahashi S, Boku S, Takahashi K, Furukawa K, Arai F, Asakura H. Enhanced expression of interleukin-6 in chronic hepatitis C. *Liver* 1999;19:464–72.
21. Jinushi M, Takehara T, Tatsumi T, Kanto T, Groh V, Spies T, Kimura R, Miyagi T, Mochizuki K, Sasaki Y, Hayashi N. Expression and role of MICA and MICB in human hepatocellular carcinomas and their regulation by retinoic acid. *Int J Cancer* 2003;104:354–61.
22. Kohga K, Takehara T, Tatsumi T, Ishida H, Miyagi T, Hosui A, Hayashi N. Sorafenib inhibits the shedding of MICA on hepatocellular cacrcinoma cell by downregulating ADAM9. *Hepatology* 2010; 51:1264–73.
23. Champsaur M, Lanier LL. Effect of NKG2D ligand expression on host immune responses. *Immunol Rev* 2010;235:267–85.

PLOS ONE

Functional Characterization of Domains of IPS-1 Using an Inducible Oligomerization System

Shiori Takamatsu[1,2], Kazuhide Onoguchi[1], Koji Onomoto[3], Ryo Narita[1], Kiyohiro Takahasi[1,4], Fumiyoshi Ishidate[5], Takahiro K. Fujiwara[5], Mitsutoshi Yoneyama[3], Hiroki Kato[1,2], Takashi Fujita[1,2]*

1 Laboratory of Molecular Genetics, Institute for Virus Research, Kyoto University, Kyoto, Japan, **2** Laboratory of Molecular Cell Biology, Graduate School of Biostudies, Kyoto University, Kyoto, Japan, **3** Division of Molecular Immunology, Medical Mycology Research Center, Chiba University, Chuo-ku, Chiba, Japan, **4** Institute for Innovative NanoBio Drug Discovery and Development, Graduate School of Pharmaceutical Science, Kyoto University, Kyoto, Japan, **5** Center for Meso-Bio Single-Molecule Imaging (CeMI), Institute for Integrated Cell-Material Sciences (WPI-iCeMS), Kyoto University, Kyoto, Japan

Abstract

The innate immune system recognizes viral nucleic acids and stimulates cellular antiviral responses. Intracellular detection of viral RNA is mediated by the Retinoic acid inducible gene (RIG)-I Like Receptor (RLR), leading to production of type I interferon (IFN) and pro-inflammatory cytokines. Once cells are infected with a virus, RIG-I and MDA5 bind to viral RNA and undergo conformational change to transmit a signal through direct interaction with downstream CARD-containing adaptor protein, IFN-β promoter stimulator-1 (IPS-1, also referred as MAVS/VISA/Cardif). IPS-1 is composed of N-terminal Caspase Activation and Recruitment Domain (CARD), proline-rich domain, intermediate domain, and C-terminal transmembrane (TM) domain. The TM domain of IPS-1 anchors it to the mitochondrial outer membrane. It has been hypothesized that activated RLR triggers the accumulation of IPS-1, which forms oligomer as a scaffold for downstream signal proteins. However, the exact mechanisms of IPS-1-mediated signaling remain controversial. In this study, to reveal the details of IPS-1 signaling, we used an artificial oligomerization system to induce oligomerization of IPS-1 in cells. Artificial oligomerization of IPS-1 activated antiviral signaling without a viral infection. Using this system, we investigated the domain-requirement of IPS-1 for its signaling. We discovered that artificial oligomerization of IPS-1 could overcome the requirement of CARD and the TM domain. Moreover, from deletion- and point-mutant analyses, the C-terminal Tumor necrosis factor Receptor-Associated Factor (TRAF) binding motif of IPS-1 (aa. 453–460) present in the intermediate domain is critical for downstream signal transduction. Our results suggest that IPS-1 oligomerization is essential for the formation of a multiprotein signaling complex and enables downstream activation of transcription factors, Interferon Regulatory Factor 3 (IRF3) and Nuclear Factor-κB (NF-κB), leading to type I IFN and pro-inflammatory cytokine production.

Citation: Takamatsu S, Onoguchi K, Onomoto K, Narita R, Takahasi K, et al. (2013) Functional Characterization of Domains of IPS-1 Using an Inducible Oligomerization System. PLoS ONE 8(1): e53578. doi:10.1371/journal.pone.0053578

Editor: Karin E. Peterson, National Institute of Allergy and Infectious Diseases - Rocky Mountain Laboratories, United States of America

Received July 21, 2012; **Accepted** November 30, 2012; **Published** January 7, 2013

Funding: The Ministry of Education, Culture, Sports, Science and Technology in Japan (Innovative Areas "Infection competency" (No.24115004), Scientific Research "A"(23249023) (http://www.mext.go.jp/english/), the Ministry of Health, Labor and Welfare of Japan (http://www.mhlw.go.jp/english/index.html), the PRESTO Japan Science and Technology Agency (http://www.jst.go.jp/kisoken/presto/index_e.html), the Uehara Memorial Foundation (http://www.ueharazaidan.com/), the Takaeda Science Foundation (http://www.takeda-sci.or.jp/index.html), the Naito Foundation (http://www.naito-f.or.jp/), and Nippon Boehringer Ingelheim (http://www.boehringer-ingelheim.co.jp/com/Home/index.jsp). The funders had no role in study design, data collection and analysis, decision to publish, or preparation of the manuscript.

Competing Interests: The authors have the following interests: This study was partly funded by Nippon Boehringer Ingelheim. There are no patents, products in development or marketed products to declare. This does not alter the authors' adherence to all the PLOS ONE policies on sharing data and materials, as detailed online in the guide for authors.

* E-mail: tfujita@virus.kyoto-u.ac.jp

Introduction

Viruses replicating within cells produce RNA with a non-self signature, such as a double stranded (ds) and 5′-triphosphate structure, which are recognized by sensor molecules Retinoic acid Inducible Gene-I (RIG-I), Melanoma Differentiation Associated gene 5 (MDA5), and Laboratory of Genetics and Physiology 2 (LGP2), collectively known as RIG-I-Like Receptors (RLR) [1,2,3,4]. RLR elicits signals to activate a set of genes including those of type I and III interferon (IFN) to initiate innate antiviral responses [5]. Several lines of evidence support a hypothesis that once RIG-I and MDA5 recognize non-self RNA, conformational changes are induced resulting in exposure of their CARD [6]. The CARD of RIG-I and MDA5 transmits a signal to another CARD-containing adaptor, Interferon Promoter Stimulator-1 (IPS-1, also known as MAVS, VISA, and Cardif), which is anchored on the outer membrane of the mitochondrion [7,8,9,10]. Cells infected with a virus activate the RLR/IPS-1 signaling cascade and exhibit microscopic aggregation of IPS-1 [11]. Activation of IPS-1 is reconstituted in vitro and the formation of detergent-insoluble IPS-1 aggregate has been reported [12]. For intracellular aggregation of IPS-1, the involvement of mitofusin (MFN) 1, which is known to regulate mitochondrial fusion, has been reported [11], suggesting that IPS-1 aggregation is regulated through a complex mechanism of mitochondrial dynamics. There are several studies concerning how IPS-1 receives a signal from RLR and how it relays it downstream; however, some of the reports are not consistent with each other [10,13,14,15]. IPS-1 contains three potential TRAF binding motifs (TBMs) [10]. To avoid confusion, we refer to them as TBM1 (aa. 143–147, human),

TBM2 (aa. 154–159, human), and TBM3 (aa. 453–460, human). TBM1 and 2 are close to each other (5 amino acids apart) and reside within the proline-rich domain. TBM1 physically interacts with TRAF3 [16] and a single amino acid substitution (T147I) abolishes binding. Early reports demonstrated that an artificial molecule essentially consisting of CARD and TM, therefore devoid of TBMs (termed mini MAVS), is sufficient for signaling [9,10,13]. In particular, TM can be replaced with that of other mitochondrial proteins, suggesting the importance of its mitochondrial localization. Other reports have demonstrated that artificial oligomerization of CARD of IPS-1 in the cytosol is sufficient to activate the signal independent of the mitochondrion [14].

In the current study, we aimed to delineate the inconsistencies on the reported function of IPS-1 domains with a focus on the oligomerization of IPS-1 and analyzed the necessary part of IPS-1 for signaling.

Results

Forced IPS-1 Oligomerization Activates Antiviral Innate Immunity

Previously, we found that a virus-infection resulted in the redistribution of IPS-1 to form speckle-like aggregates in cells [11]. Here, we attempted to demonstrate whether oligomerization of IPS-1 was sufficient to induce antiviral signaling. To address this question, we modified an artificial homodimerization system (ARGENT Kit, ARIAD) [17]. We used 3 tandem repeats of mutant FK 506 Binding Protein 12 (FK_{F36V}), which can be cross-linked by a cell-permeable chemical AP20187 (Figure 1A). FK_{F36V} harbors an F36V mutation, which impairs binding affinity to immunosuppressive agent, FK506. AP20187 was designed specifically for binding with FK_{F36V}, so that it does not influence endogenous FK binding proteins. Thus, this system specifically crosslinks a target protein without the unwanted side effects. We made constructs to artificially oligomerize CARD of RIG-I in cells (FK-RIG CARD) [18] and IPS-1 (FK-IPS) (Figure 1A). HeLa cells stably expressing $3xFK_{F36V}$ (FK) and its fusion proteins were treated with AP20187 and IFN-β mRNA levels were quantified. AP20187 induced oligomerization of fusion proteins (Native PAGE, data not shown). Oligomerization of FK_{F36V} did not induce IFN-β mRNA; however, FK-RIG CARD exhibited a rapid induction of IFN-β mRNA (Figure 1B, [18]). Two independent HeLa clones expressing FK-IPS activated the IFN-β gene upon AP20187 treatment, both of which expressed the fusion protein localized to mitochondria (data not shown). Furthermore, AP20187 treatment induced speckle-like distribution of FK-IPS in cells (data not shown). It is important to note that unlike transient overexpression of IPS-1 in cell lines, which constitutively activates the IFN-β gene; stable cells did not exhibit constitutive IFN-β expression (Figure 1B). To confirm that this induction was accompanied by activation of IRF-3, its dimer formation was examined by native PAGE (Figure 1C). Consistent with IFN-β mRNA levels, cells expressing FK-RIG and FK-IPS, but not FK exhibited rapid IRF-3 dimer formation after exposure to AP20187.

To further confirm the impact of antiviral signaling by this artificial system, we examined expression profiles of interferon stimulated genes by a DNA microarray of 237 immune-related genes. 109 genes were transiently induced by IPS-1 oligomer (data not shown). Representatives 11 genes, which are known to be induced after a viral infection, are displayed in Figure 1D. Results show that a simple oligomerization of FK-RIG CARD or FK-IPS mimics the signaling induced by a viral infection (Figure 1D). In contrast, only CARD of IPS-1 failed to induce any interferon or cytokine gene expression in response to oligomerization (Figure S1). From this, it would appear that the up-regulations of these genes are not due to non-specific response induced by oligomerized CARD-containing protein.

CARD of IPS-1 is Dispensable for Oligomerization-induced Signaling

It has been hypothesized that upon activation of RIG-I, its CARD is exposed by conformational changes and relays signaling to IPS-1 through CARD-CARD interactions [8,9,10,19]. CARD of IPS-1 is essential for signaling when IPS-1 is transiently overexpressed [7,8]. We examined if CARD of IPS-1 was essential in FK-IPS-mediated signaling. We constructed FK-IPS mutants: FK-IPSΔCARD, CARD deletion; FK-IPSCARD, FK fused to CARD; FK-IPSTM, FK fused to TM, and FK-IPSΔCARDΔTM, FK-IPS without CARD and TM, as summarized in Figure 2A. Stable cells expressing FK-IPSΔCARD showed little basal activation of IRF-3; upon treatment with AP20187, strong activation of IRF-3 was observed similar to that by FK-IPS (Figure 2B). However, FK-IPS CARD did not activate IRF-3 even after oligomerization (Figure 2B). Similarly, FK-IPSΔCARD, but not FK-IPSCARD did not induce IFN-β mRNA upon oligomerization (Figure 2C). Oligomerization of FK on the mitochondrion (FK-IPSTM) is not sufficient to activate IFN-β and Interleukin(IL)-6 genes (Figure 2D, 2E). Interestingly, FK-IPSΔCARDΔTM, which is localized in the cytoplasm (Figure S2) due to TM deletions, activated IFN-β and IL-6 genes and formed speckle-like aggregates upon oligomerization (Figure 2D, 2E, and Figure S2). These results suggest that cytoplasmic oligomerization of an IPS-1 fragment (aa. 90–507), which includes TBM1–3, is sufficient for signaling and mitochondrial localization is dispensable if forcibly oligomerized.

Domain Delimitation of IPS-1 for IRF3 and NF-κB Activation

To delimit the region of IPS-1 necessary to trigger signaling upon oligomerization, we made a series of deletion mutants as shown in Figure 3A. Stable clones of HeLa cells expressing these mutants were mock treated or treated with AP20187 and nuclear translocation of IRF-3 and NF-κB was determined by immunostaining (Figure 3B). Deletion of the proline-rich region (180–540) showed little effect; however, further deletion of residues 400 to 464 abolished activation of both IRF-3 and NF-κB, indicating that these residues are essential to signal. Quantitative analysis of IFN-β and IL-6 gene expression revealed a significant attenuation of signaling by the deletion of aa. 1–179 (Figure 3C, 3D), suggesting the involvement of TBM1 and 2. This requirement of TBM1–2 is more prominent for IL-6 gene expression. Importantly, further deletion of aa. 400 to 464 (FK_{F36V}-IPS 465–540), including TBM3, resulted in the complete loss of signaling activity.

We also wondered whether MFN1 contributes to IPS-1 oligomerization because we previously reported that mitochondrial protein MFN1 promotes mitochondrial fusion and increases signaling of IPS-1 [11]. We carried out a reporter assay with this oligomerization system in MFN1−/− MEFs. MFN1−/− MEFs showed comparable level of IFN-promoter activity to WT MEF cells (Figure S3), suggesting that MFN1 is dispensable for signaling induced by forced oligomerization of IPS-1.

Essential Role of TBM3 in Signaling

To further characterize functional residues within aa. 400–540, we substituted a single amino acid within TBM3 (PEENEY to

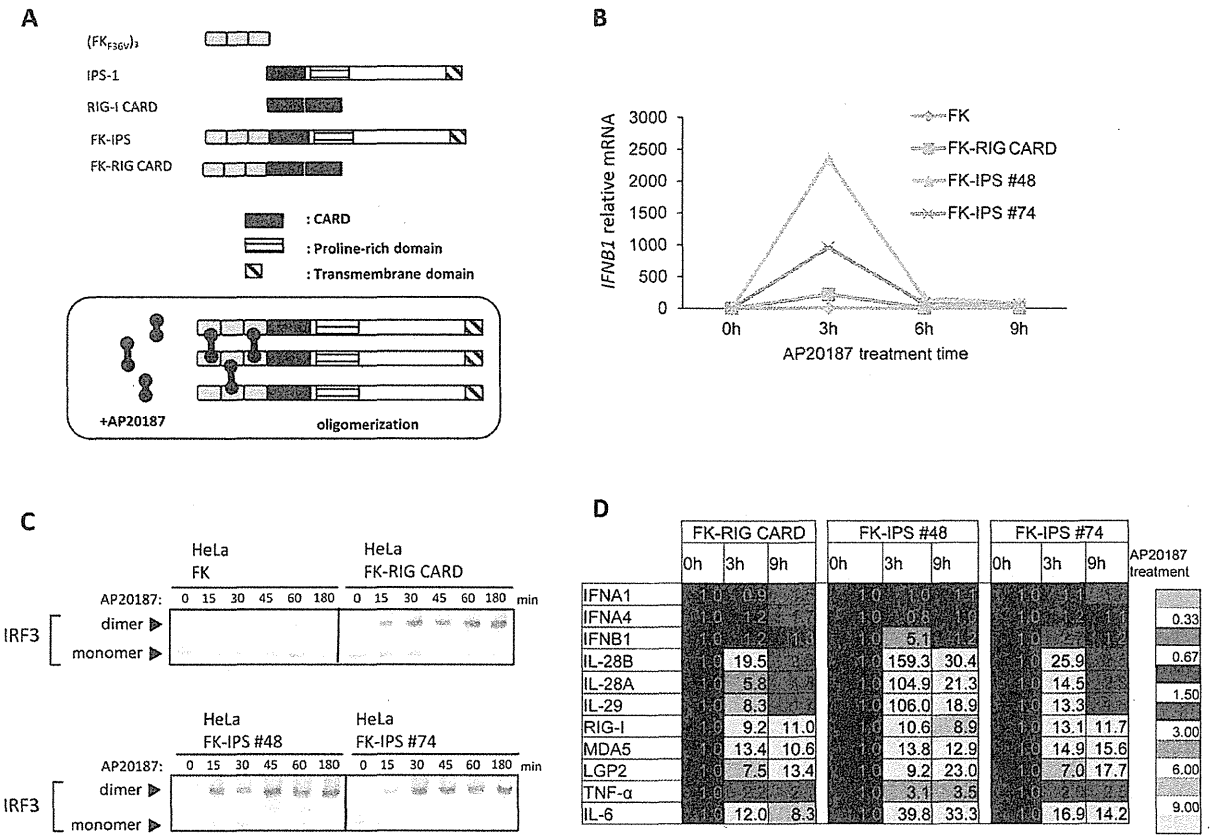

Figure 1. Forced IPS-1 oligomerization induced antiviral innate immune signaling. A. Schematic representation of FKBP fusion proteins and their oligomerization by a cross-linker, AP20187. B. HeLa cells stably expressing indicated FKBP fusion proteins were treated with AP20187 (10 nM) for the indicated time. Cells were harvested and analyzed for IFN-β mRNA levels by qPCR. C. HeLa cells stably expressing indicated FKBP fusion proteins were stimulated with AP20187 for 3 h and IRF-3 dimer formation was analyzed (Materials and Methods). Positions of the IRF-3 monomer and dimer are shown by arrowheads. D. Microarray analysis of mRNAs induced by oligomerized RIG-I CARD or IPS-1. Cells were stimulated with AP20187 for the indicated time. Total RNA extracted from these cells was subjected to analysis using a DNA microarray (Genopal, Mitsubishi Rayon) of interferon-stimulated genes and interferon genes. Relative mRNA levels using a control expression as 1.0 are shown. Representative data of at least two independent experiments are shown.
doi:10.1371/journal.pone.0053578.g001

PEDNEY: E457D) [10] to explore its significance (Figure 4A). E457D substitution abolished gene activation of IFN-β and IL-6 with full-length or 400–540 FK_{F36V} fusion constructs in stable HeLa cells (Figure 4B, 4C). We confirmed that IRF and NF-κB were activated by oligomerization of IPS-1 400–540 in a TBM3-dependent manner (Figure 4D, 4E). We further mutagenized TBM3 to resemble TBM of Toll/IL-1 receptor domain-containing adaptor inducing IFN-β (TRIF) (PEEMSW) or IL-1 receptor-associated kinase (IRAK)-M (PVEDDE). As a negative control, the motif was replaced to that of Myeloid Differentiation factor 88 (MyD88) (PSILRF), which does not bind directly to the TRAF molecule [20]. Interestingly, substitution of TBM3 with TBM of TRIF or IRAK-M restored the induction of IRF3 and NF-κB, albeit with lower efficiency (Figure 4F, 4G). As expected, the control motif of MyD88 failed to exhibit signaling. Furthermore, we constructed FK-IPS 400–508, which retains TBM3 but lacks the TM. This short fragment of IPS-1 also activated IRF-responsive promoter upon oligomerization(Figure S4). This result further supports the hypothesis that oligomerization of TBM3 is essential in IPS-1 mediated signaling.

Viral Infection Induces Molecular Oligomer of IPS-1

The above results show that forced oligomerization of IPS-1 results in the activation of a signaling cascade. We investigated if a viral infection induced oligomerization of IPS-1 using fusion proteins of complementary fragments of a fluorescent reporter protein (monomeric Kusabira-Green, mKG) [21]. Two split inactive mKG fragments fused to IPS-1, respectively, were expressed in cells. Fluorescence is expected to be detectable when these IPS-1 fusions containing complementary mKG fragment came into close vicinity (Figure 5A). 293T cells, which stably expressed mKG-fusion IPS-1, were infected with Newcastle disease virus (NDV) for 9h and then subjected to Fluorescence-Activated Cell Sorting (FACS) analysis for the detection of fluorescence. We observed enhanced fluorescence in NDV-infected cells (Figure 5B), suggesting that viral infections induce oligomer formation of IPS-1.

Discussion

Signaling initiated by cytoplasmic viral RNA sensors involves a unique adaptor, IPS-1, which is specifically expressed on the outer

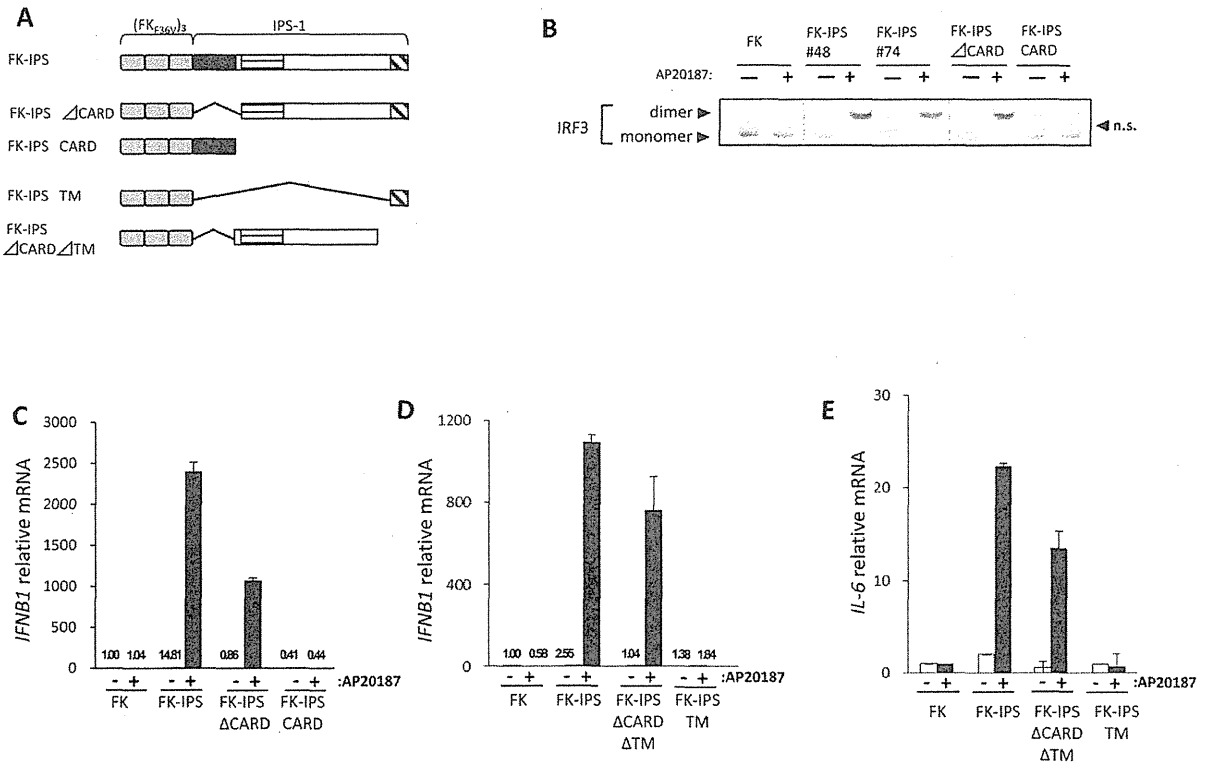

Figure 2. CARD of IPS-1 is dispensable for oligomerization-induced signaling. A. Schematic representation of FK-IPS deletion mutants. B. HeLa cells stably expressing indicated FK-IPS fusion were mock treated or treated with AP20187 for 3 h. Cell lysates were analyzed for IRF-3 dimer formation as in Figure 1C. n.s.: non-specific band. C–E. Indicated HeLa cells stably expressing FK-IPS constructs were mock treated or treated with AP20187 for 3 h. Cellular RNA were extracted and analyzed for IFN-β (C, D) or Il-6 (E) mRNA by qPCR. Representative data of at least two independent experiments are shown. Error bars: standard error of triplicated samples.
doi:10.1371/journal.pone.0053578.g002

membrane of the mitochondrion. IPS-1 is a problematic protein, since transient overexpression results in constitutive signaling, whereas endogenous IPS-1 is tightly regulated by post-translational mechanisms [22,23]. Here, we established a system to analyze the regulation of IPS-1 by its oligomerization. We obtained stable cell lines expressing FK-IPS fusion, which could be activated by a crosslinker. Upon oligomerization, IPS-1 rapidly elicited signaling leading to the activation of target genes including that of IFN-β, suggesting that IPS-1 aggregation is essential and precedes possible covalent modifications such as phosphorylation and ubiquitination [24,25].

Our deletion analysis of FK-IPS-1 revealed that the TRAF binding motif is essential while CARD is dispensable for signaling. The initial report by Chen's group reported that CARD tethered to mitochondria-targeted TM (termed mini MAVS) is sufficient to transduce signaling by its transient overexpression [9,13]. They expressed mini-MAVS in cells expressing endogenous IPS-1. However, when mini-MAVS was expressed in IPS-1−/− cells, no signal was transduced (Figure S5, [26]). And recently Chen's group also reported that depletion of endogenous IPS-1 by RNAi abrogated interferon induction by mini-MAVS [12]. This can be interpreted as transient overexpression of CARD in the vicinity of mitochondria resulting in the aggregation of endogenous IPS-1. In contrast, FK-IPS 400–450, which lacks CARD, is regulated by oligomerization in IPS-1−/− MEFs (Figure 4D, 4E). Another group showed that cytoplasmic oligomerization of CARD is sufficient to activate signaling using FK fusion [14]. This result is clearly inconsistent with ours (Figure 2B, 2C). They used wild type FKBP12 and dimerizer chemical AP1510, which retains its binding affinity to endogenous FKBP proteins. One of the FKBPs, FKBP38 (also termed FKBP8) is known to associate with the mitochondrial outer membrane [27]. Therefore, this primordial oligomerization system may oligomerize the target proteins (this case CARD) in association with mitochondria. We used an improved FKBP system (ARGENT Kit, ARIAD), which avoids this potential problem. On the other hand, FK-IPS ΔCARDΔTM, which contains TBMs, can activate signaling upon oligomerization (Figure 2). This result highlights the fact that cytoplasmic oligomerization of TBMs is sufficient for signaling.

There are three potential TBMs within IPS-1 [10]. Our result showing that FK-IPS 400–540 exhibited signaling in an oligomerization-dependent manner (Figures 3 and 4) suggest that oligomerization of TBM 3 alone is sufficient for signaling. TBM3, initially identified as TRAF6 binding site [10], can also recruit TRAF3 [28]. This is consistent with studies using TRAF3 and TRAF6 knockout cells [29,30]. TBM1, 2, and 3 likely contribute to the signaling mediated by IPS-1, presumably in a cooperative fashion and result in differential activation of target genes. For example, TBM1 and 2 are dispensable for the IFN-β gene, but IL-6 gene requires all TBM1, 2, and 3 for full activation (Figure 3C, 3D). A recent report has shown that CARD containing protein CARD9 is preferentially required for

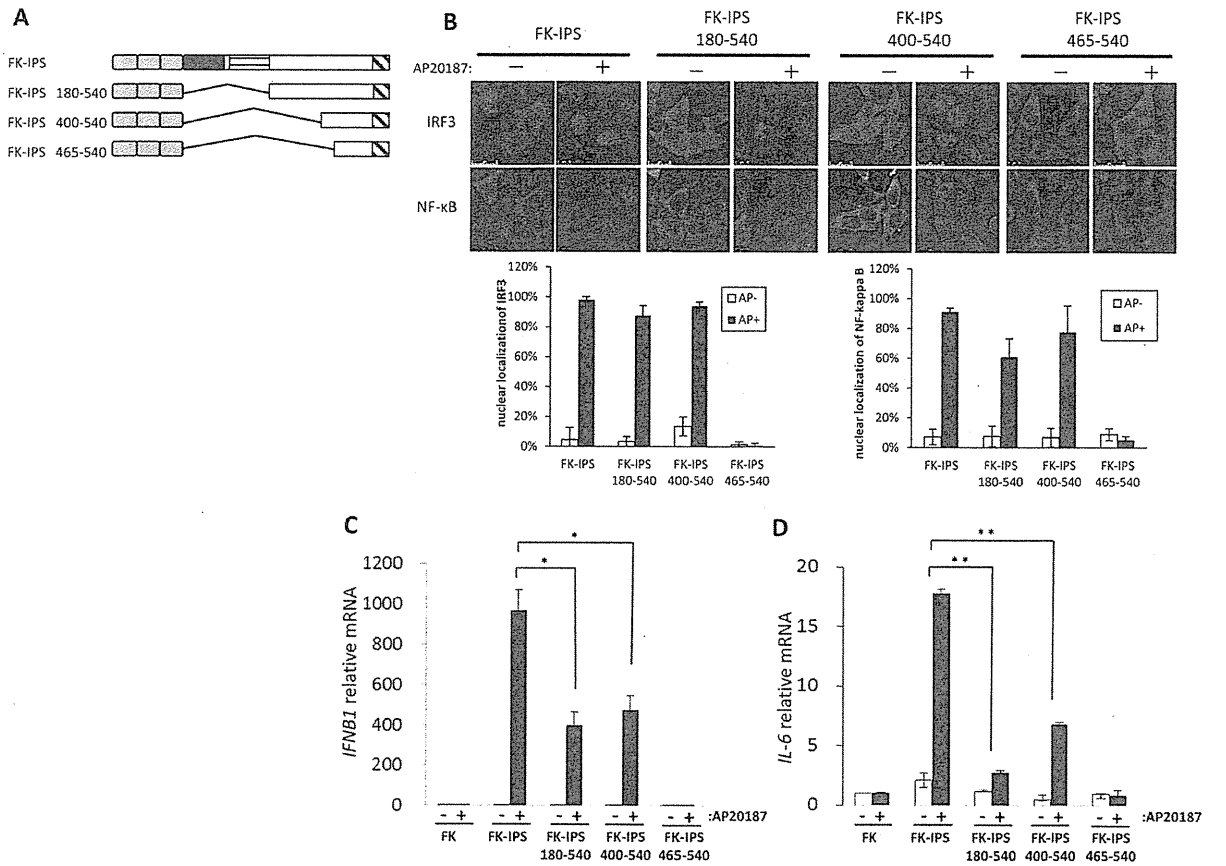

Figure 3. Delimitation of critical domain in IPS-1 for IRF3 and NF-κB activation. A. Schematic representation of FK-IPS deletion mutants. B. HeLa cells stably expressing indicated FK-IPS deletion mutants were mock treated or treated with AP20187 for 3 h. Cell were fixed and stained for IRF-3 and NF-κB p65, respectively. Fluorescent microscopic images of IRF3 and NF-κB staining are shown (top). The percentage of cells with nuclear IRF-3 or NF-κB was determined by counting 100 cells (bottom). C, D. Cellular RNA was extracted and analyzed for IFN-β (C) or IL-6 (D) mRNA by qPCR. Representative data of at least two independent experiments are shown. Error bars: standard error of triplicated samples. Statistical analyses were conducted with an unpaired t test, with values of $p<0.05$ considered statistically significant. *$p<0.05$, **$p<0.005$.
doi:10.1371/journal.pone.0053578.g003

proinflammatory cytokine induction downstream of RIG-I signaling [31]. To explore the involvement of CARD9 in IPS-1 mediated signaling, we knocked down CARD9 in a stable HeLa clone expressing FK-IPS and examined its effect on the activation of IFN-β and IL-6 genes (Figure S7). Although IFN-β gene induction by oligomerization was little affected by reducing CARD9, IL-6 gene activation was significantly attenuated. Considering the result that IL-6 gene activation is more dependent on TBM1/2 (Figure 3C, 3D), it is tempting to speculate that TBM1/2 preferentially promote NF-κB activation, whereas TBM3 has a primary role of IRF-3/7 activation.Our results support a model that CARD of IPS-1 receives signaling from RLR via CARD-CARD interaction to initiate oligomerization through mitochondrial dynamism; however, CARD of IPS-1 alone is not sufficient to trigger downstream signaling. On the other hand, TBMs are essential for further signaling by the recruitment of TRAF3 and 6, which is initiated by molecular oligomerization. Consistent with this model, we observed that artificial oligomerization of IPS-1 induced recruitment of TRAF6 into the NP-40-insoluble fraction (Figure S6). Thus, IPS-1 receives and transmits signaling through the functions of CARD and the TRAF motif, respectively.

Materials and Methods

Plasmid Constructs

p-55C1BLuc, p-55A2Luc, p-125Luc, pRLtk, pEF-Bos-FLAG-RIG-I CARD and pEF-Bos-FLAG-IPS-1 plasmids have been described [11,32]. Expression plasmids of FKBP36v (oligomerization peptide), pC4M-Fv2E, and pC4Fv1E were obtained from ARIAD (ARGENT Regulated Homodimerization kit). We reconstructed the vector, pC4Fv3E, which contains 3 tandem repeats of FKBP36v [18]. To construct IPS-1 fused three tandem FKBP, we amplified the IPS-1 sequence by PCR and inserted it into the SpeI site of pC4Fv3E. Site-directed FK-fused IPS-1 mutants (FK-IPS E457D, FK-IPS 400–540 E457D) were constructed using a KOD-Plus mutagenesis kit (TOYOBO, Japan). Nucleotide sequences for these constructs were confirmed with the BigDye DNA sequencing kit (Applied Biosystems). Expression vectors encording Flag-MAVS and Flag-mini-MAVS were obtained from Dr. Zhijian J. Chen.

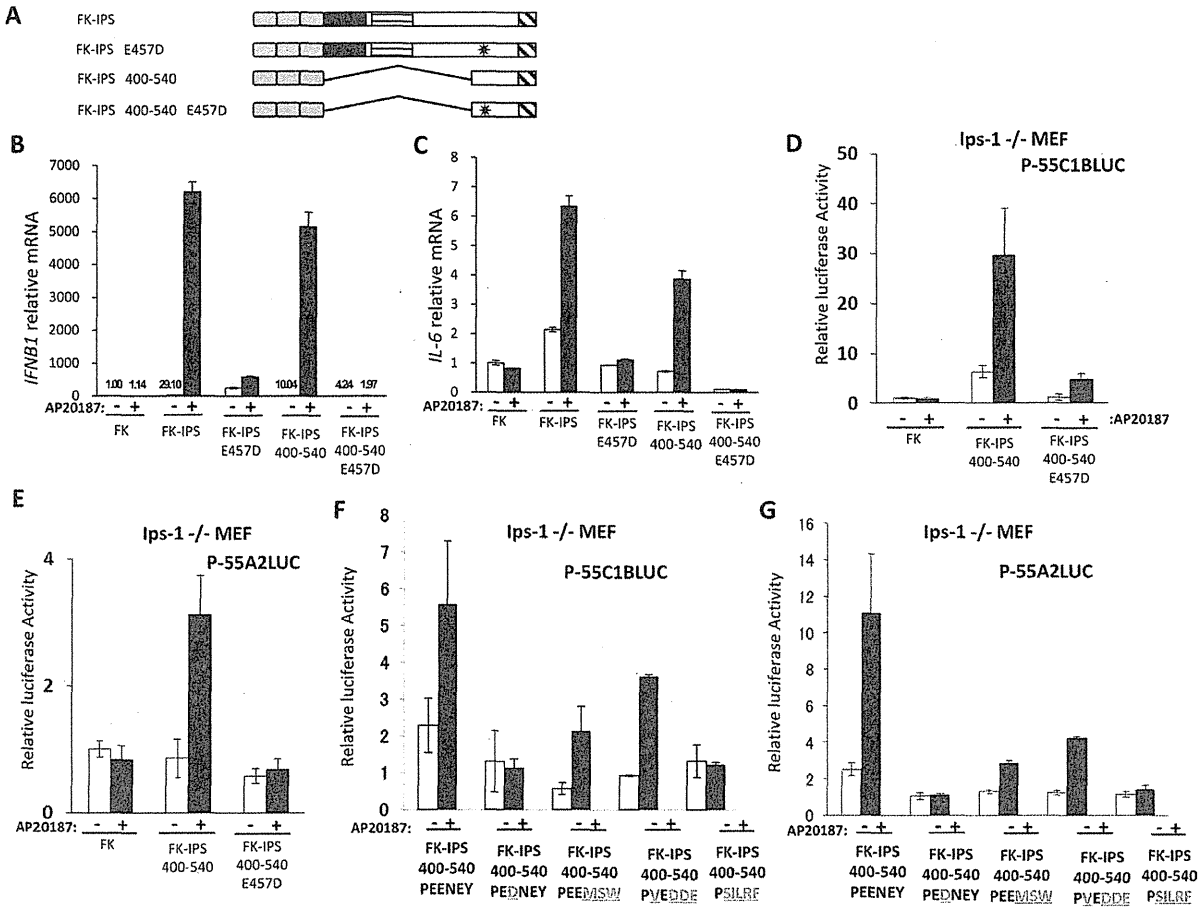

Figure 4. Essential role of TBM3 in signaling. A. Schematic representation of FK-IPS fusion proteins. Asterisks represent the point mutation. B, C. HeLa cells stably expressing indicated FK-IPS mutants were mock treated or treated with AP20187 for 3 h. Cellular RNA were extracted and analyzed for IFN-β (B) or IL-6 (C) mRNA by qPCR. D–G. IPS-1−/− MEFs were transiently transfected with the luciferase reporter plasmid, p-55C1BLuc (for IRF, D, F) or p-55A2Luc (for NF-κB, E, G), together with indicated FK-IPS-1 fusion constructs. For TBM3 mutants, substituted amino acids are shown as red letters (F, G). Cells were treated with or without AP20187 for 6 h. Relative luciferase activities were determined as described in the Materials and Methods. A representative result of at least two independent experiments is shown. Error bars: standard error of triplicated samples.
doi:10.1371/journal.pone.0053578.g004

Cell, DNA Transfection, and Preparation of Cell Extracts

HeLa, 293T cells [32,33] and Mouse embryonic fibroblasts (MEFs) [5,34] were maintained in Dulbecco's Modified Eagle's Medium with 10% fetal bovine serum and penicillin-streptomycin. MEFs deficient for IPS-1 were obtained from Dr. S. Akira (Osaka University). MEFs deficient in MFN1 were obtained from Dr. David Chan (Caltech). HeLa, 293T cells, and MEFs were transfected with FuGENE 6 (Roche Applied Science). Stable transformants of HeLa cells were established by transfection of linearized plasmids, encoding the FKBP construct and Puromycin resistance gene, respectively, and cells were selected by Puromycin (5 μg/ml). For preparation of cell extracts, cells were lysed with lysis buffer (50 mM Tris-HCl pH 7.5, 150 mM NaCl, 1 mM EDTA, 1% Nonidet P-40, 0.1 mg/ml leupeptin, 1 mM phenylmethylsulfonyl fluoride, and 1 mM sodium orthovanadate) and were centrifuged at 20400×g for 10 min. The supernatant was used for immunoblotting.

Viral Unfection

Cells were treated with culture medium or infected with NDV at a MOI of 1 in serum-free and antibiotic-free medium. After adsorption for 1 h at 37°C, the medium was changed and infection was continued for 9 h in the precence of serum-containing medium.

Reporter Assay

MEFs were transfected with firefly luciferase reporter (either p-125 Luc, p-55C1BLuc or p-55A2Luc [32]) pRLtk (renilla luciferase internal control) and effector expression plasmids. Cells were split into three aliquots and were stimulated with chemical dimerizer AP20187 (AP, 10 ng/ml in ethanol) or ethanol. The luciferase assay was performed with a Dual-Luciferase reporter assay system (Promega). Luciferase activity was normalized using *Renilla* luciferase activity (pRLtk).

Quantitative Real Time PCR and Microarray Analysis

Total RNA was prepared with TRIZOL reagent (Invitrogen) and treated with DNase I (Roche Diagnostics). A High-Capacity

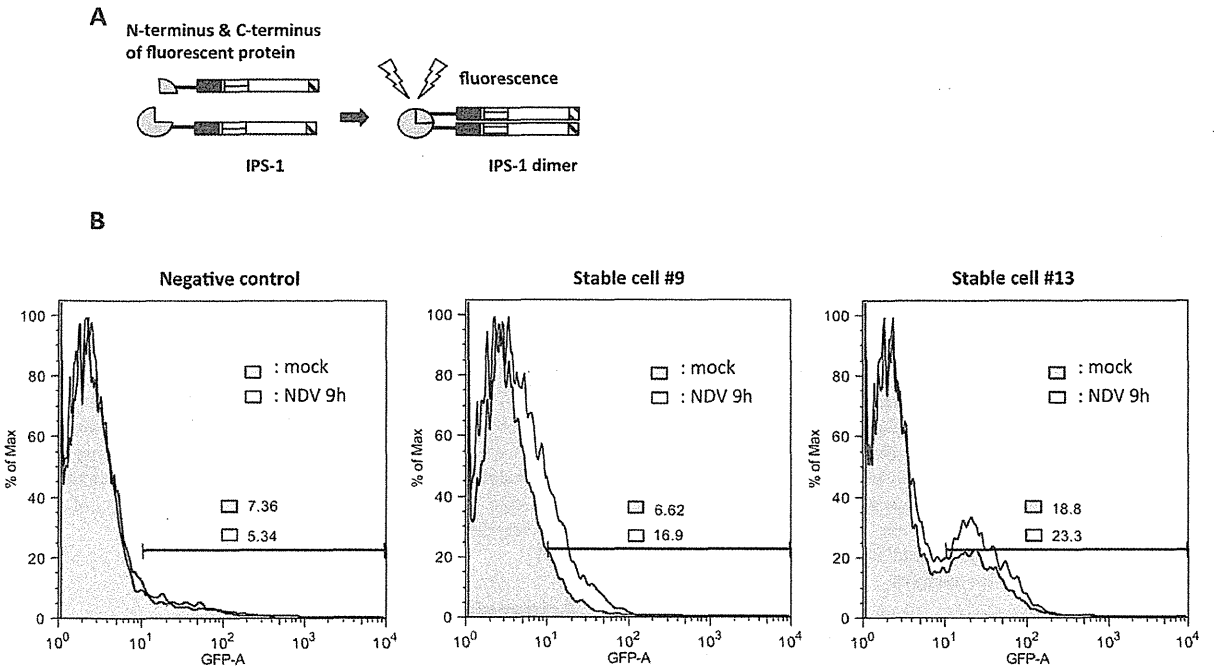

Figure 5. Viral infection induces the molecular oligomer of IPS-1. A. Schematic representation of dimers detection by mKG-tagged IPS-1. B. Flow cytometry plots of control 293T cells and 2 clones stably expressing mKG-tagged IPS-1, #9 and #13. The cells were mock treated or infected with NDV for 9 h. Cells exhibiting fluorescent intensity $>10^1$ were quantified and expressed as % of total cell number.
doi:10.1371/journal.pone.0053578.g005

cDNA Reverse Transcription Kit (Applied Biosystems) was used for cDNA synthesis and mRNA levels were monitored with the Step One plus Real Time PCR system and TaqMan Fast Universal PCR Master Mix (Applied Biosystems). TaqMan primer-probes for human IFNB1, IL-6, IFNA8, and 18 s rRNA were purchased from Applied Biosystems. RNA copy numbers were normalized to that of an internal 18 s rRNA. In the microarray analysis, we used the Genopal microarray system according to the manufacturer's instructions (Mitsubishi Rayon). Biotin-labeled RNA was prepared with a MessageAmp II-Biotin Enhanced kit (Ambion).

Immunoblotting and Antibodies

The polyclonal antibody used to detect human IRF-3 in native PAGE and anti-human IRF-3 polyclonal antibodies for immunostaining were described previously [35]. Other antibodies were obtained from the following sources: Anti-human NF-κB antibody (sc-109), anti-human TRAF6 (sc-8409), and anti-human MFN1 (sc-50330) from Santa Cruz Biotechnology, anti-HA-Tag (6E2) from Cell Signaling, and anti-human Actin (A-1978) from Sigma.

Immunofluorescence Microscopy

For immunofluorescence analysis, cells were fixed with 4% paraformaldehyde for 10 min, permeabilized with acetone: methanol (1:1), and blocked with 5 mg/ml of BSA in PBST (0.04% Teen20 in PBS) for 1hour. Cells were incubated with relevant primary antibodies overnight at 4°C, then incubated with Alexa Fluor-conjugated secondary antibodies (Invitrogen). To label mitochondria, cells were incubated for 30 min at 37°C with MitoTracker Red CMXRos according to the manufacturer's instructions (Molecular Probes). Fluorescence images were obtained by Leica Microsystems AF6500 (Leica).

RNA Interference

The siRNA negative control, targeting TRAF3 and TRAF6 were purchased from Bonac Corporation. The target sequences were: (GCUCAUGGAUGCUGUGCAUdTdT) and (GGAGAAACCUGUUGUGAUUdTdT) for TRAF3 and 6, respectively. Each siRNA was transfected with Lipofectamine 2000 (Invitrogen) according to the manufacturer's instructions. At 48 h post-transfection, cells were harvested, and then subjected to Real Time PCR.

FACS

To examine oligomerization of IPS-1 in cells, we performed bimolecular fluorescence complementation (BiFC) assays using a CoralHue Fluo-Chase kit (Amalgam).

293T cells expressing this construct were washed and harvested with PBS, then subjected to FACS analysis using FACSCanto II (BD Bioscience).

Supporting Information

Figure S1 Microarray analysis of mRNAs induced by oligomerized IPS-1 CARD or IPS-1. HeLa cells stably expressing FK-IPS or FK-IPS CARD were stimulated with AP20187 for the indicated time. Total RNA extracted from these cells was subjected to analysis using a DNA microarray (Genopal, Mitsubishi Rayon) of interferon-stimulated genes and interferon genes. Relative mRNA levels using a control expression as 1.0 are shown.
(PDF)

Figure S2 FK-IPS ΔCARDΔTM forms speckle like aggregates in the cytoplasm. HeLa cells stably expressing FK-IPS ΔCARDΔTM were mock treated or treated with

AP20187 for 3 h and stained with mitoTracker (mitochondria) and anti-HA antibody. Fluorescent microscopic images of FK-IPSΔCARDΔTM and mitochondria are shown.
(PDF)

Figure S3 MFN1 is dispensable for signaling induced by forced oligomerization of IPS-1. MEFs of MFN1−/− or +/+ were transiently transfected with p-125Luc (reporter for IFN-β promoter activity) together with the indicated FK-IPS fusion constructs. Cells were treated with or without AP20187 for 6 h. Relative luciferase activities were determined as described in Materials and Methods. A representative result of at least two independent experiments is shown. Error bars indicate standard error of triplicate samples.
(PDF)

Figure S4 FK-IPS 400–508 can activate IRF-responsive promoter upon oligomerization. HEK 293T cells were transiently transfected with p-55C1BLuc together with the FK or FK-IPS 400–540 constructs. Cells were treated with or without AP20187 for 6 h. Relative luciferase activities were determined as described in Materials and Methods. A representative result of at least two independent experiments is shown. Error bars indicate standard error of triplicate samples.
(PDF)

Figure S5 IPS-1Δ100–500 (mini-MAVS) failed to activate signaling in the absence of endogenous IPS-1. IPS-1−/− or +/+ MEFs were transiently transfected with luciferase reporter plasmid, p-55C1BLuc together with IPS-1(MAVS), IPS-1Δ100–500 (mini-MAVS), or control vector. Relative luciferase activities were determined as described in Materials and Methods. A representative result of at least two independent experiments is shown. Error bars indicate standard error of triplicate samples.
(PDF)

Figure S6 Recruitment of TRAF6 into NP-40 insoluble fraction upon oligomerization of IPS-1. A. Scheme for isolation of soluble and insoluble fractions by differential centrifugation. **B and C.** Immunoblot analysis of soluble/insoluble fractions separated by differential centrifugation. FK-IPS ΔCARD stable cells were cultured for 3 h in the absence or presence of AP. Cell lysates were separated by differential centrifugation. FK-IPS ΔCARD and endogenous MFN1, TRAF6, and actin were detected by immunoblotting.
(PDF)

Figure S7 Involvement of CARD9 in NF-κB dependent pathway. A. HeLa FK-IPS#48 cells were transfected with N.C. siRNA or CARD9 targeted siRNA for 48 h, and the knockdown of CARD9 was analyzed by RT-PCR. **B, C and D.** HeLa FK-IPS#48 cells were transfected with N.C. siRNA or CARD9 targeted siRNA for 48 h, then mock treated or treated with AP20187 for 3 h. Cellular RNA were extracted and analyzed for IFN-β (B), Il-6 (C) or Il-1β (D) mRNA by qPCR. Representative data of at least two independent experiments are shown. Error bars: standard error of triplicated samples. Statistical analyses were conducted with an unpaired t test, with values of $p<0.05$ considered statistically significant. *$p<0.05$.
(PDF)

Acknowledgments

We are grateful to S. Akira for the IPS-1 deficient MEFs, Z. J. Chen for the plasmid constructs, and D. Chan for MFN1 deficient MEFs.

Author Contributions

Conceived and designed the experiments: ST K. Onoguchi K. Onomoto MY TF. Performed the experiments: ST K. Onoguchi K. Onomoto RN FI TKF. Analyzed the data: ST K. Onoguchi K. Onomoto RN KT FI MY HK TF TKF. Wrote the paper: ST K. Onoguchi K. Onomoto RN MY HK TF.

References

1. Yoneyama M, Kikuchi M, Natsukawa T, Shinobu N, Imaizumi T, et al. (2004) The RNA helicase RIG-I has an essential function in double-stranded RNA-induced innate antiviral responses. Nat Immunol 5: 730–737.
2. Yoneyama M, Kikuchi M, Matsumoto K, Imaizumi T, Miyagishi M, et al. (2005) Shared and unique functions of the DExD/H-box helicases RIG-I, MDA5, and LGP2 in antiviral innate immunity. J Immunol 175: 2851–2858.
3. Pichlmair A, Schulz O, Tan CP, Naslund TI, Liljestrom P, et al. (2006) RIG-I-mediated antiviral responses to single-stranded RNA bearing 5′-phosphates. Science 314: 997–1001.
4. Hornung V, Ellegast J, Kim S, Brzozka K, Jung A, et al. (2006) 5′-Triphosphate RNA is the ligand for RIG-I. Science 314: 994–997.
5. Onoguchi K, Yoneyama M, Takemura A, Akira S, Taniguchi T, et al. (2007) Viral infections activate types I and III interferon genes through a common mechanism. J Biol Chem 282: 7576–7581.
6. Sambhara S, Fujita T (2012) Nucleic Acid Sensors and Antiviral Immunity. Austin (TX): Landes Bioscience.
7. Kawai T, Takahashi K, Sato S, Coban C, Kumar H, et al. (2005) IPS-1, an adaptor triggering RIG-I- and Mda5-mediated type I interferon induction. Nat Immunol 6: 981–988.
8. Meylan E, Curran J, Hofmann K, Moradpour D, Binder M, et al. (2005) Cardif is an adaptor protein in the RIG-I antiviral pathway and is targeted by hepatitis C virus. Nature 437: 1167–1172.
9. Seth RB, Sun L, Ea CK, Chen ZJ (2005) Identification and characterization of MAVS, a mitochondrial antiviral signaling protein that activates NF-kappaB and IRF 3. Cell 122: 669–682.
10. Xu LG, Wang YY, Han KJ, Li LY, Zhai Z, et al. (2005) VISA is an adapter protein required for virus-triggered IFN-beta signaling. Mol Cell 19: 727–740.
11. Onoguchi K, Onomoto K, Takamatsu S, Jogi M, Takemura A, et al. (2010) Virus-infection or 5′ppp-RNA activates antiviral signal through redistribution of IPS-1 mediated by MFN1. PLoS Pathog 6: e1001012.
12. Hou F, Sun L, Zheng H, Skaug B, Jiang QX, et al. (2011) MAVS forms functional prion-like aggregates to activate and propagate antiviral innate immune response. Cell 146: 448–461.
13. Li XD, Sun L, Seth RB, Pineda G, Chen ZJ (2005) Hepatitis C virus protease NS3/4A cleaves mitochondrial antiviral signaling protein off the mitochondria to evade innate immunity. Proc Natl Acad Sci U S A 102: 17717–17722.
14. Tang ED, Wang CY (2009) MAVS self-association mediates antiviral innate immune signaling. J Virol 83: 3420–3428.
15. Tang ED, Wang CY (2010) TRAF5 is a downstream target of MAVS in antiviral innate immune signaling. PLoS One 5: e9172.
16. Saha SK, Pietras EM, He JQ, Kang JR, Liu SY, et al. (2006) Regulation of antiviral responses by a direct and specific interaction between TRAF3 and Cardif. EMBO J 25: 3257–3263.
17. Clackson T, Yang W, Rozamus LW, Hatada M, Amara JF, et al. (1998) Redesigning an FKBP-ligand interface to generate chemical dimerizers with novel specificity. Proc Natl Acad Sci U S A 95: 10437–10442.
18. Ouda R, Onomoto K, Takahasi K, Edwards MR, Kato H, et al. (2011) Retinoic acid-inducible gene I-inducible miR-23b inhibits infections by minor group rhinoviruses through down-regulation of the very low density lipoprotein receptor. J Biol Chem 286: 26210–26219.
19. Yoneyama M, Fujita T (2010) Recognition of viral nucleic acids in innate immunity. Rev Med Virol 20: 4–22.
20. Ye H, Arron JR, Lamothe B, Cirilli M, Kobayashi T, et al. (2002) Distinct molecular mechanism for initiating TRAF6 signalling. Nature 418: 443–447.
21. Ueyama T, Kusakabe T, Karasawa S, Kawasaki T, Shimizu A, et al. (2008) Sequential binding of cytosolic Phox complex to phagosomes through regulated adaptor proteins: evaluation using the novel monomeric Kusabira-Green System and live imaging of phagocytosis. J Immunol 181: 629–640.
22. Belgnaoui SM, Paz S, Hiscott J (2011) Orchestrating the interferon antiviral response through the mitochondrial antiviral signaling (MAVS) adapter. Curr Opin Immunol 23: 564–572.
23. Koshiba T (2012) Mitochondrial-mediated antiviral immunity. Biochim Biophys Acta.
24. Lin R, Heylbroeck C, Pitha PM, Hiscott J (1998) Virus-dependent phosphorylation of the IRF-3 transcription factor regulates nuclear translocation, transactivation potential, and proteasome-mediated degradation. Mol Cell Biol 18: 2986–2996.

25. Mao AP, Li S, Zhong B, Li Y, Yan J, et al. (2010) Virus-triggered ubiquitination of TRAF3/6 by cIAP1/2 is essential for induction of interferon-beta (IFN-beta) and cellular antiviral response. J Biol Chem 285: 9470–9476.
26. Paz S, Vilasco M, Arguello M, Sun Q, Lacoste J, et al. (2009) Ubiquitin-regulated recruitment of IkappaB kinase epsilon to the MAVS interferon signaling adapter. Mol Cell Biol 29: 3401–3412.
27. Shirane M, Nakayama KI (2003) Inherent calcineurin inhibitor FKBP38 targets Bcl-2 to mitochondria and inhibits apoptosis. Nat Cell Biol 5: 28–37.
28. Paz S, Vilasco M, Werden SJ, Arguello M, Joseph-Pillai D, et al. (2011) A functional C-terminal TRAF3-binding site in MAVS participates in positive and negative regulation of the IFN antiviral response. Cell Res 21: 895–910.
29. Oganesyan G, Saha SK, Guo B, He JQ, Shahangian A, et al. (2006) Critical role of TRAF3 in the Toll-like receptor-dependent and -independent antiviral response. Nature 439: 208–211.
30. Yoshida R, Takaesu G, Yoshida H, Okamoto F, Yoshioka T, et al. (2008) TRAF6 and MEKK1 play a pivotal role in the RIG-I-like helicase antiviral pathway. J Biol Chem 283: 36211–36220.
31. Poeck H, Bscheider M, Gross O, Finger K, Roth S, et al. (2010) Recognition of RNA virus by RIG-I results in activation of CARD9 and inflammasome signaling for interleukin 1 beta production. Nat Immunol 11: 63–69.
32. Yoneyama M, Suhara W, Fukuhara Y, Fukuda M, Nishida E, et al. (1998) Direct triggering of the type I interferon system by virus infection: activation of a transcription factor complex containing IRF-3 and CBP/p300. EMBO J 17: 1087–1095.
33. Daly C, Reich NC (1993) Double-stranded RNA activates novel factors that bind to the interferon-stimulated response element. Mol Cell Biol 13: 3756–3764.
34. Kumar H, Kawai T, Kato H, Sato S, Takahashi K, et al. (2006) Essential role of IPS-1 in innate immune responses against RNA viruses. J Exp Med 203: 1795–1803.
35. Iwamura T, Yoneyama M, Yamaguchi K, Suhara W, Mori W, et al. (2001) Induction of IRF-3/−7 kinase and NF-kappaB in response to double-stranded RNA and virus infection: common and unique pathways. Genes Cells 6: 375–388.

HEPATOLOGY
Official Journal of the American Association for the Study of Liver Diseases

Hepatitis C Virus NS4B Protein Targets STING and Abrogates RIG-I–Mediated Type I Interferon-Dependent Innate Immunity

Sayuri Nitta,[1*] Naoya Sakamoto,[1,2,6*] Mina Nakagawa,[1,2] Sei Kakinuma,[1,2] Kako Mishima,[1] Akiko Kusano-Kitazume,[1] Kei Kiyohashi,[1] Miyako Murakawa,[1] Yuki Nishimura-Sakurai,[1] Seishin Azuma,[1] Megumi Tasaka-Fujita,[1] Yasuhiro Asahina,[1,2] Mitsutoshi Yoneyama,[3] Takashi Fujita,[4,5] and Mamoru Watanabe[1]

Hepatitis C virus (HCV) infection blocks cellular interferon (IFN)-mediated antiviral signaling through cleavage of Cardif by HCV-NS3/4A serine protease. Like NS3/4A, NS4B protein strongly blocks IFN-β production signaling mediated by retinoic acid–inducible gene I (RIG-I); however, the underlying molecular mechanisms are not well understood. Recently, the stimulator of interferon genes (STING) was identified as an activator of RIG-I signaling. STING possesses a structural homology domain with flaviviral NS4B, which suggests a direct protein-protein interaction. In the present study, we investigated the molecular mechanisms by which NS4B targets RIG-I–induced and STING-mediated IFN-β production signaling. IFN-β promoter reporter assay showed that IFN-β promoter activation induced by RIG-I or Cardif was significantly suppressed by both NS4B and NS3/4A, whereas STING-induced IFN-β activation was suppressed by NS4B but not by NS3/4A, suggesting that NS4B had a distinct point of interaction. Immunostaining showed that STING colocalized with NS4B in the endoplasmic reticulum. Immunoprecipitation and bimolecular fluorescence complementation (BiFC) assays demonstrated that NS4B specifically bound STING. Intriguingly, NS4B expression blocked the protein interaction between STING and Cardif, which is required for robust IFN-β activation. NS4B truncation assays showed that its N terminus, containing the STING homology domain, was necessary for the suppression of IFN-β promoter activation. NS4B suppressed residual IFN-β activation by an NS3/4A-cleaved Cardif (Cardif1-508), suggesting that NS3/4A and NS4B may cooperate in the blockade of IFN-β production. *Conclusion*: NS4B suppresses RIG-I–mediated IFN-β production signaling through a direct protein interaction with STING. Disruption of that interaction may restore cellular antiviral responses and may constitute a novel therapeutic strategy for the eradication of HCV. (HEPATOLOGY 2013;57:46-58)

Type I interferon (IFN) plays a central role in eliminating hepatitis C virus (HCV) both under physiological conditions and when used as a therapeutic intervention.[1-3] In experimental acute-resolving HCV infection in chimpanzees, numerous IFN-related genes are expressed during clinical course of infection.[4] Viruses are recognized by cellular innate immune receptors, such as toll-like receptors, and a family of RIG-I–like receptors, such as retinoic-acid-inducible gene I (RIG-I) and melanoma-differentiation-associated gene 5 (MDA-5); host antiviral responses are then activated, resulting in the

From the [1]Departments of Gastroenterology and Hepatology; [2]Departments of Hepatitis Control, Tokyo Medical and Dental University, Tokyo, Japan; [3]Division of Molecular Immunology, Medical Mycology Research Center, Chiba University, Chiba, Japan; [4]Laboratory of Molecular Genetics, Department of Genetics and Molecular Biology, Institute for Virus Research, Kyoto University, Kyoto, Japan; [5]Laboratory of Molecular Cell Biology, Graduate School of Biostudies, Kyoto University, Kyoto, Japan; and [6]Department of Gastroenterology and Hepatology, Hokkaido University, Hokkaido, Japan.

Received September 16, 2011; accepted July 24, 2012.

BiFC, bimolecular fluorescence complementation; CARD, caspase recruitment domain; DAPI, 4',6-diamidino-2-phenylindole; dsRNA, double-stranded RNA; ER, endoplasmic reticulum; FACL4, fatty acid-CoA ligase, long chain 4; HCV, hepatitis C virus; IFN, interferon; IKKε, IκB kinase ε; IRF-3, interferon-regulatory factor 3; ISRE, interferon-stimulated response element; MAM, mitochondria-associated ER membrane; mKG, monomeric Kusabira-Green; PDI, protein disulphide-isomerase; pIRF-3, phosphorylated IRF3; poly(dA:dT), poly(deoxyadenylic-deoxythymidylic) acid; RIG-I, retinoic acid–inducible gene I; siRNA, small interfering RNA; SOCS, suppressor of cytokine signaling; STAT1, signal transducer and activator of transcription protein-1; STING, stimulator of interferon genes; TBK1, TANK binding kinase 1.

**These authors contributed equally to this work.*

production of cytokines such as type I and type III IFNs.[5] RIG-I is activated through recognition of short double-strand RNA (dsRNA) or triphosphate at the 5′ end of dsRNA as pathogen-associated molecular patterns,[6,7] forming a homo-oligomer that binds with the caspase recruitment domain (CARD) of Cardif (also known as MAVS, VISA, or IPS-1).[8-11] Cardif subsequently recruits TANK binding kinase 1 (TBK1) and IκB kinase ϵ (IKKϵ) kinases, which catalyze phosphorylation and activation of IFN regulatory factor-3 (IRF-3).[12] Activation of TBK1 and IKKϵ results in the phosphorylation of IRF-3 or IRF-7, translocation to the nucleus, and induction of IFN-β mRNA transcription.

Several HCV proteins can block host cellular antiviral responses. HCV core protein blocks IFN signaling by interacting with signal transducer and activator of transcription protein-1 (STAT1).[13] The core protein also induces expression of suppressor of cytokine signaling-1 (SOCS1) and SOCS3, and blocks Janus kinase–STAT signaling.[14,15] A well-elucidated immune evasion strategy of HCV involves NS3/4A serine protease and its ability to inhibit host IFN signal pathways. Gale and colleagues[11,16,17] revealed that NS3/4A protease cleaves Cardif at Cys-508 resulting in dislocation of Cardif from mitochondria, and blocks downstream signaling of IFN-β production. On the other hand, Baril et al.[18] reported that Cardif was still able to form a homo-oligomer and to activate downstream IFN production signaling despite delocalization from the mitochondria. These reports suggest that homo-oligomerization of Cardif, and not mitochondrial anchorage, is essential for the activation of downstream IFN signaling and that other virus-derived molecules may cooperate with NS3/4A to abrogate the signaling of IFN production.

We reported previously that HCV-NS4B, as well as NS3/4A, inhibited RIG-I and Cardif-mediated interferon-stimulated response element (ISRE) activation, while TBK1- and IKKϵ-mediated ISRE activation were not suppressed.[19] These results indicate that NS4B suppresses IFN production signaling by targeting Cardif or other unknown signaling molecules between the level of Cardif and TBK1/IKKϵ.

Recently, a stimulator of interferon genes (STING, also known as MITA/ERIS/MPYS/TMEM173) was identified as a positive regulator of RIG-I–mediated IFN-β signaling.[20-23] STING is a 42-kDa protein localized predominantly in the endoplasmic reticulum (ER) that binds RIG-I, Cardif, TBK1, and IKKϵ. STING is thought to act as a scaffold for Cardif/TBK1/IRF-3 complex upon viral infection.[22] It has been reported that NS4B of yellow fever virus, which is a member of the flaviviridae family of viruses, inhibits its STING activation probably through a direct molecular interaction.[24] These reports have led us postulate that HCV-NS4B may also inhibit RIG-I dependent IFN signaling through association with STING.

In the present study, we further investigated the molecular mechanisms by which HCV-NS4B protein inhibits RIG-I–mediated IFN expression signaling. We demonstrated that HCV-NS4B specifically binds STING, blocks the molecular interaction between STING and Cardif, and suppresses the RIG-I–like receptor–induced activation of IFN-β production signaling.

Materials and Methods

Plasmids. The ΔRIG-I and RIG-IKA plasmids express constitutively active and inactive RIG-I, respectively.[5] Full-length Cardif (Cardif) and CARD-truncated Cardif (ΔCARD) plasmids were provided by J. Tschopp.[11] Plasmids expressing STING were provided by G. N. Barber.[20] Plasmids expressing HCV NS3/4A, NS4B, and truncated NS4B have been described.[25] Plasmid pIFNβ-Fluc was provided by R. Lin.[26]

Cell Culture. HEK293T and Huh7 cells were maintained in Dulbecco's modified minimal essential medium (Sigma) supplemented with 2 mM L-glutamine and 10% fetal calf serum at 37°C with 5% CO_2.

HCV Replicon Constructs and HCV-JFH1 Cell Culture. An HCV subgenomic replicon plasmid, pRep-Feo, expressed fusion protein of firefly luciferase and neomycin phosphotransferase.[27,28] Huh7 cells were transfected by Rep-Feo RNA, cultured in the presence of 500 μg/mL of G418, and a cell line that stably expressed Feo replicon was established. For HCV cell culture, the HCV-JFH1 strain was used.[29,30]

Antibodies. Antibodies used were anti–IRF-3 (FL-425, Santa Cruz Biotechnology), anti-HA (Invitrogen), anti-myc (Invitrogen), mouse anti-PDI (Abcam),

Address reprint requests to: Naoya Sakamoto, M.D., Ph.D., Department of Gastroenterology and Hepatology, Hokkaido University, Kita15, Nishi8, Kita-ku, Sapporo, Hokkaido, 060-0808, Japan. E-mail: nsakamoto.gast@tmd.ac.jp; fax (81)-11-706-8036.

View this article online at wileyonlinelibrary.com.

DOI 10.1002/hep.26017

Potential conflict of interest: Nothing to report.

Additional Supporting Information may be found in the online version of this article.

rabbit anti-PDI (Enzo Life Science), anti-Flag (Sigma Aldrich), anti-Cardif (Enzo Life Science), anti-phospho–IRF-3 (Ser396, Millipore), anti-monomeric Kusabira-Green C- or N-terminal fragment (MBL), and anti-FACL4 (Abgent).

Luciferase Reporter Assay. IFN-β reporter assays were performed as described.[19,31] The plasmids pIFN-β-Fluc and pRL-CMV were cotransfected with NS3/4A or NS4B, and ΔRIG-I, Cardif, STING or poly(deoxyadenylic-deoxythymidylic) acid [poly(dA:dT)] (Invivogen). RIG-IKA, ΔCARD, and pcDNA3.1, respectively, were used as controls. Luciferase assays were performed 24 hours after transfection by using a 1420 Multilabel Counter (ARVO MX PerkinElmer) and Dual Luciferase Assay System (Promega). Assays were performed in triplicate, and the results are expressed as the mean ± SD.

Immunoblotting. Preparation of total cell lysates was performed as described.[19,28] Protein was separated using NuPAGE 4%-12% Bis/Tris gels (Invitrogen) and blotted onto an Immobilon polyvinylidene difluoride membrane. The membrane was immunoblotted with primary followed by secondary antibody, and protein was detected by chemiluminescence.

Immunoprecipitation Assay. HEK-293T or Huh7 cells were transfected with plasmids as indicated. Twenty-four hours after transfection, cellular proteins were harvested and immunoprecipitation assays were performed using an Immunoprecipitation Kit according to the manufacturer's protocol (Roche Applied Science). The immunoprecipitated proteins were analyzed by immunoblotting.

Indirect Immunofluorescence Assay. Cells seeded onto tissue culture chamber slides were transfected with plasmids as indicated. Twenty-four hours after transfection, the cells were fixed with cold acetone and incubated with primary antibody and subsequently with Alexa488- or Alexa568-labeled secondary antibodies. Mitochondria were stained by MitoTracker (Invitrogen). Cells were visualized using a confocal laser microscope (Fluoview FV10, Olympus).

BiFC Assay. Expression plasmids of NS4B, Cardif, or STING that was fused with N- or C-terminally truncated monomeric Kusabira-Green (mKG) were constructed by inserting polymerase chain reaction–amplified fragments encoding NS4B, Cardif, or STING, respectively, inserted into fragmented mKG vector (Coral Hue Fluo-Chase Kit; MBL). HEK293T cells were transfected with a complementary pair of mKG fusion plasmids. Twenty-four hours after transfection, fluorescence-positive cells were detected and counted by flow cytometry, or observed by confocal laser microscopy.

Small Interfering RNA Assay. Nucleotide sequences of STING-targeted small interfering RNAs (siRNAs) were as follows: (1) 5′-gcaacagcatctatgagcttctggagaac-3′, (2) 5′- gtgcagtgagccagcggctgtatattctc;-3′, (3) 5′-gctggcat ggtcatattacatcggatatc-3′.[22] Stealth RNAi Negative Control Duplex (Medium GC Duplex, Invitrogen) was used. Forty-eight hours after siRNA transfection, expression levels of STING were detected by immunoblotting.

Statistical Analyses. Statistical analyses were performed using unpaired, two-tailed Student t test. $P < 0.05$ were considered to be statistically significant.

Results

NS4B Suppressed RIG-I, Cardif, and STING-Mediated Activation of IFN-β Expression Signaling. First, we performed a reporter assay using a luciferase reporter plasmid regulated by native IFN-β promoter. Consistent with our previous study,[19] overexpression of NS4B, as well as NS3/4A, inhibited the IFN-β promoter activation that was induced by ΔRIG-I and Cardif, respectively (Fig. 1A). We next studied whether NS4B targets STING and inhibits RIG-I pathway–mediated activation of IFN-β production. Expression of NS4B protein significantly suppressed STING-mediated activation of the IFN-β promoter reporter, whereas expression of NS3/4A showed no effect on STING-induced IFN-β promoter activity (Fig. 1A). To study whether NS4B blocks the STING-mediated DNA-sensing pathway, we performed a reporter assay using a luciferase reporter plasmid cotransfection with poly(dA:dT), which is a synthetic analog of B-DNA and has been reported to induce STING-mediated IFN-β production and NS4B. NS4B significantly blocked poly(dA:dT)-induced IFN-β promoter activation, suggesting that NS4B may block STING signaling in the DNA-sensing pathway (Fig. 1A).

Activation of RIG-I signaling induces phosphorylation of IRF-3, which is a hallmark of IRF-3 activation.[32] Thus, we examined the effects of NS3/4A and NS4B expression on phosphorylation of IRF-3 by immunoblotting analysis. As shown in Fig. 1B, overexpression of ΔRIG-I, Cardif, or STING in HEK293T cells increased levels of phosphorylated IRF-3 (pIRF-3). Expression of NS4B impaired the IRF-3 phosphorylation that was induced by ΔRIG-I, Cardif, or STING. NS3/4A also blocked production of pIRF-3 induced by ΔRIG-I or Cardif. Intriguingly, NS3/4A did not block STING-induced pIRF-3 production. These results demonstrate that both NS3/4A and

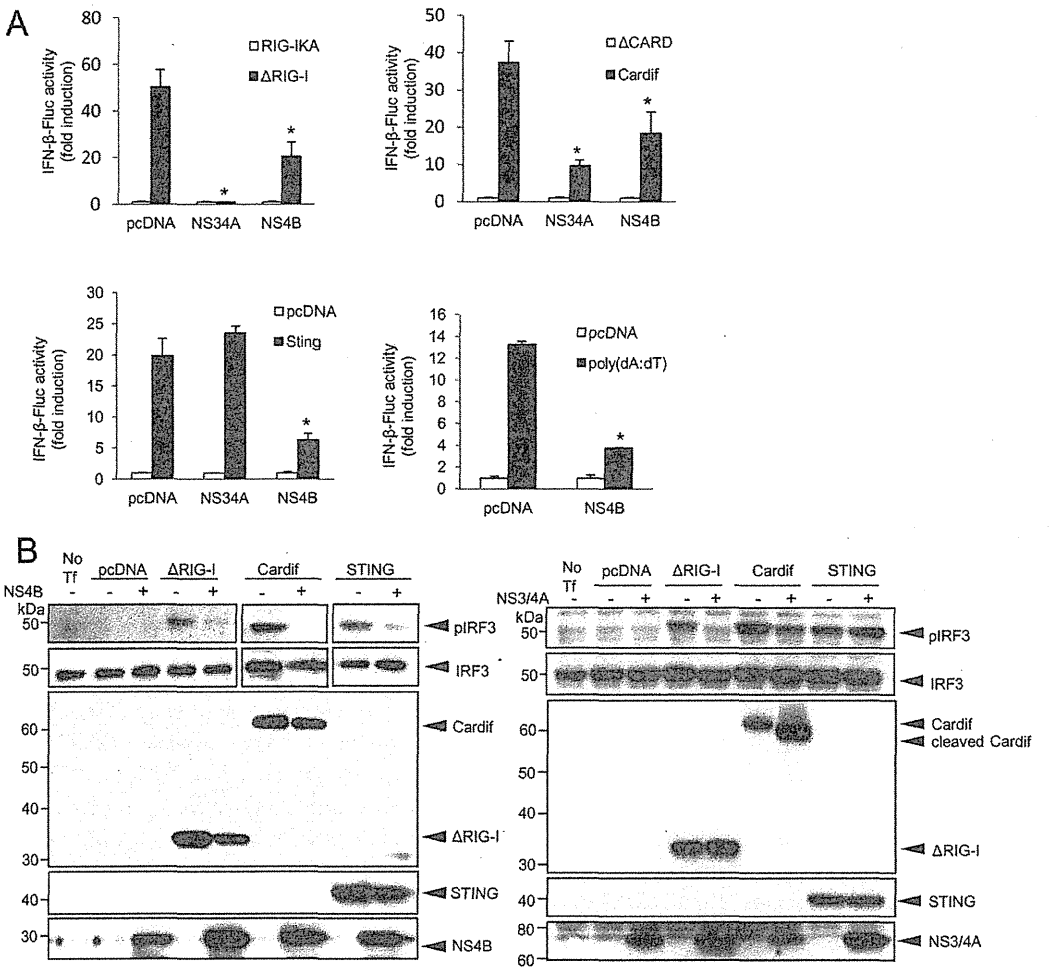

Fig. 1. NS4B suppressed IFN-β signaling mediated by RIG-I, Cardif, or STING. (A) Plasmids expressing ΔRIG-I, Cardif, or STING or poly(dA:dT) as well as NS3/4A or NS4B were cotransfected with pIFN-β-Fluc and pRL-CMV into HEK293T cells. After 24 hours, dual luciferase assays were performed. Plasmids expressing RIG-IKA, ΔCARD, or an empty plasmid (pcDNA) were used as a corresponding negative control. The experiments were performed more than three times and yielded consistent results. The *y* axis indicates relative IFN-β–Fluc activity. Assays were performed in triplicate and error bars indicate mean ± SD. $^*P < 0.05$. (B) HEK293T cells were cotransfected with indicated plasmids. On the day after transfection, the cells were lysed and immunoblot analyses were performed. No Tf, transfection-negative controls. pIRF-3 and IRF-3, phosphorylated and total IRF-3, respectively.

NS4B suppress RIG-I–mediated IFN-β production, but they do so by targeting different molecules in the signaling pathway.

Subcellular Localization of NS4B, Cardif, and STING. We next studied the subcellular localization of NS4B following its overexpression and measured the colocalization of NS4B with Cardif and STING in both HEK293T cells and Huh7 cells by indirect immunofluorescence microscopy. NS4B was localized predominantly in the ER, which is consistent with previous reports[33] (Fig. 2A). Cardif was localized in mitochondria but did not colocalize with the ER-resident host protein disulphide-isomerase (PDI). Interestingly, Cardif and NS4B colocalized partly at the boundary of the two proteins, although their original localization was different (Fig. 2A,C). STING was localized predominantly in the ER[20,21] (Fig. 2B,D). STING colocalized partly with Cardif, which is consistent with a previous report by Ishikawa and Barber[20] (Fig. 2B,D). In cells cotransfected with NS4B and STING expression plasmids, NS4B colocalized precisely with STING (Fig. 2B,D). To examine the region of NS4B-STING interaction, we next observed the two proteins by performing staining for them along with mitochondria-associated ER membrane (MAM), which is a physical association with mitochondria[34] and has been reported the site of Cardif-STING association.[24] Both NS4B and STING were adjacent to and partially colocalized

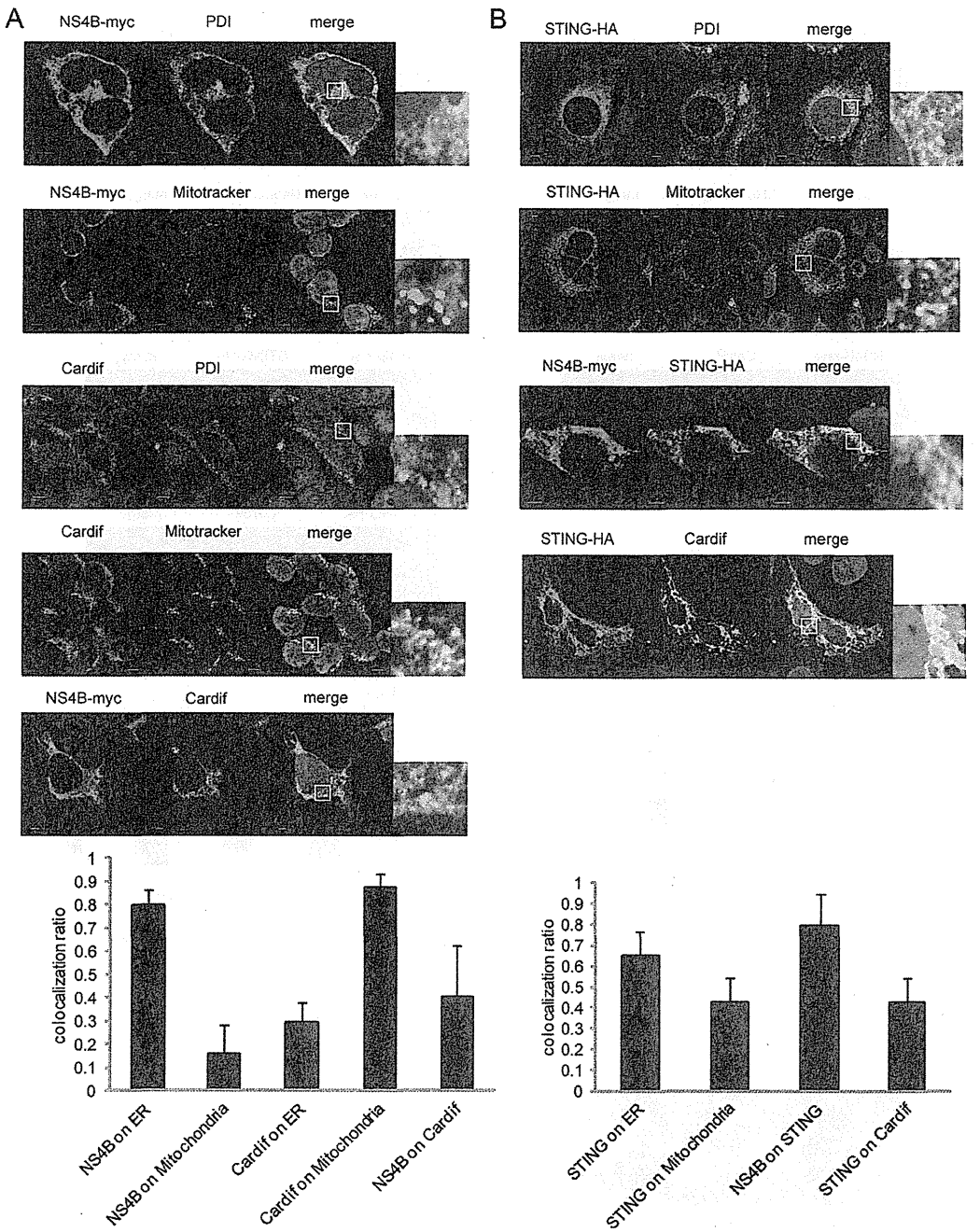

Fig. 2. Subcellular localization of NS4B, Cardif, and STING. (A-D) Subcellular localization of NS4B, Cardif, and STING in 293T (A,C) and Huh7 (B,D) cells. (A,C) NS4B-myc (first, second, and fifth panels of A and third panel of C) was transfected, and 24 hours later the cells were fixed and immunostained with anti-myc. In the third, fourth, and fifth panels of A, and the first and second panels of C, endogenous Cardif was detected with anti-Cardif antibody. ER was immunostained with anti-PDI antibody (first and third panels of A and first panel of C). Mitochondria were stained using Mitotracker (second and fourth panels of A and second panel of C). Nuclei were stained with 4',6-diamidino-2-phenylindole (DAPI). (B,D) STING-HA (all panels) and NS4B-myc (third panels) were transfected, and after 24 hours the cells were fixed and immunostained with anti-HA or anti-myc, respectively. In the fourth panels, endogenous Cardif was detected with anti-Cardif antibody. ER was immunostained with anti-PDI antibody (first panels). Mitochondria were stained using Mitotracker (second panels). Nuclei were stained with DAPI. (E) NS4B-myc and STING-HA were transfected into Huh7 cells and after 24 hours the cells were fixed and immunostained with anti-HA, anti-myc, and anti-FACL4 (MAM) antibody. Cells were visualized by confocal microscopy. Scale bars indicate 5 μm. In each microscopic image, the grade of protein colocalization in a single cell was quantified and is shown in the graphs at the bottom of each panel. Values are shown as the average colocalization ratio in 8 cells. Error bars indicate the mean + SD.

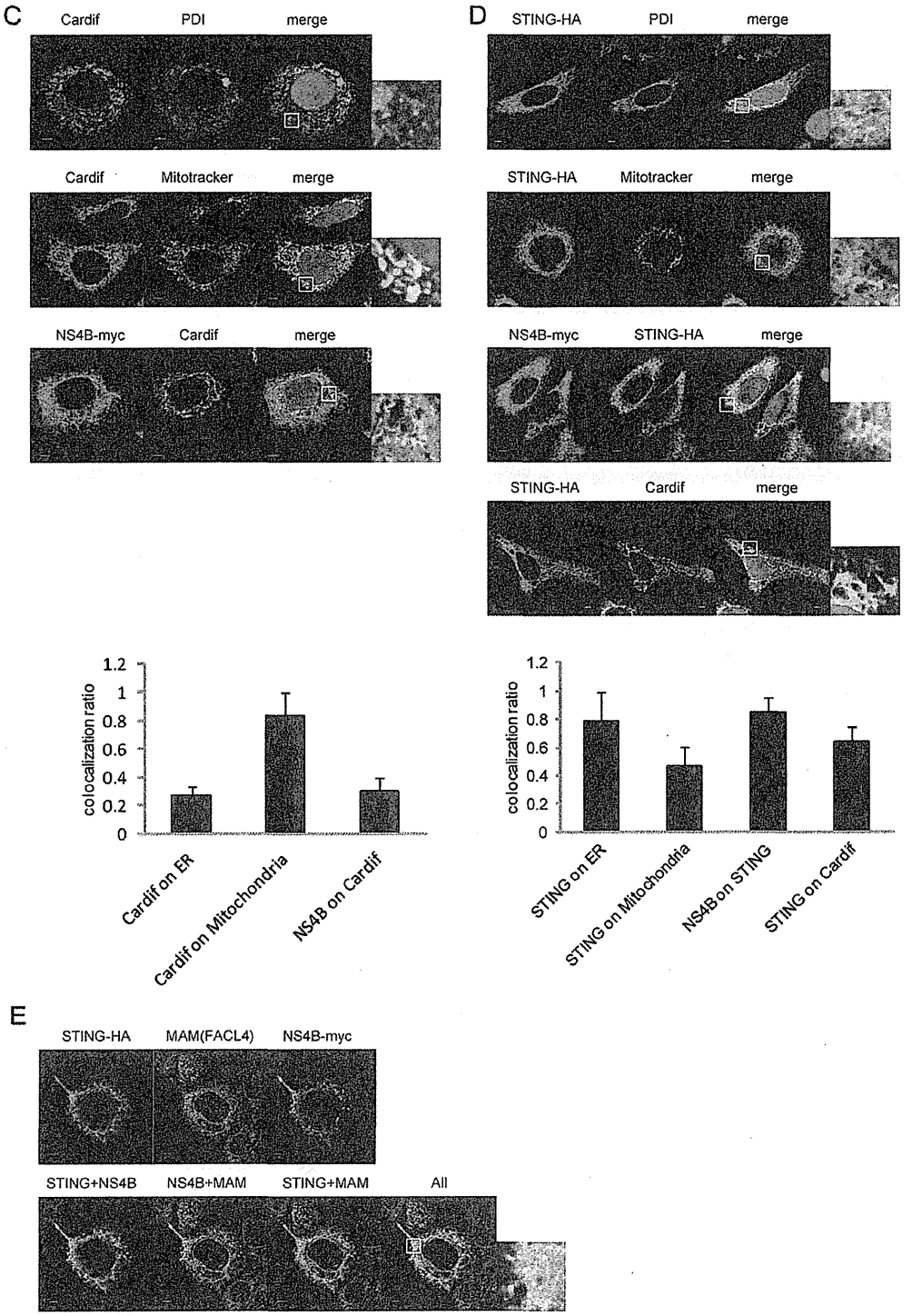

Fig. 2. Continued

with fatty acid-CoA ligase long chain 4 (FACL4), which is a MAM marker protein[35,36] (Fig. 2E). These findings suggest that NS4B might interact with STING on MAM more strongly than with Cardif.

Protein-Protein Interaction Between NS4B, Cardif, and STING. Knowing that NS4B was colocalized strongly with STING and only partly with Cardif, we next analyzed direct protein-protein interactions

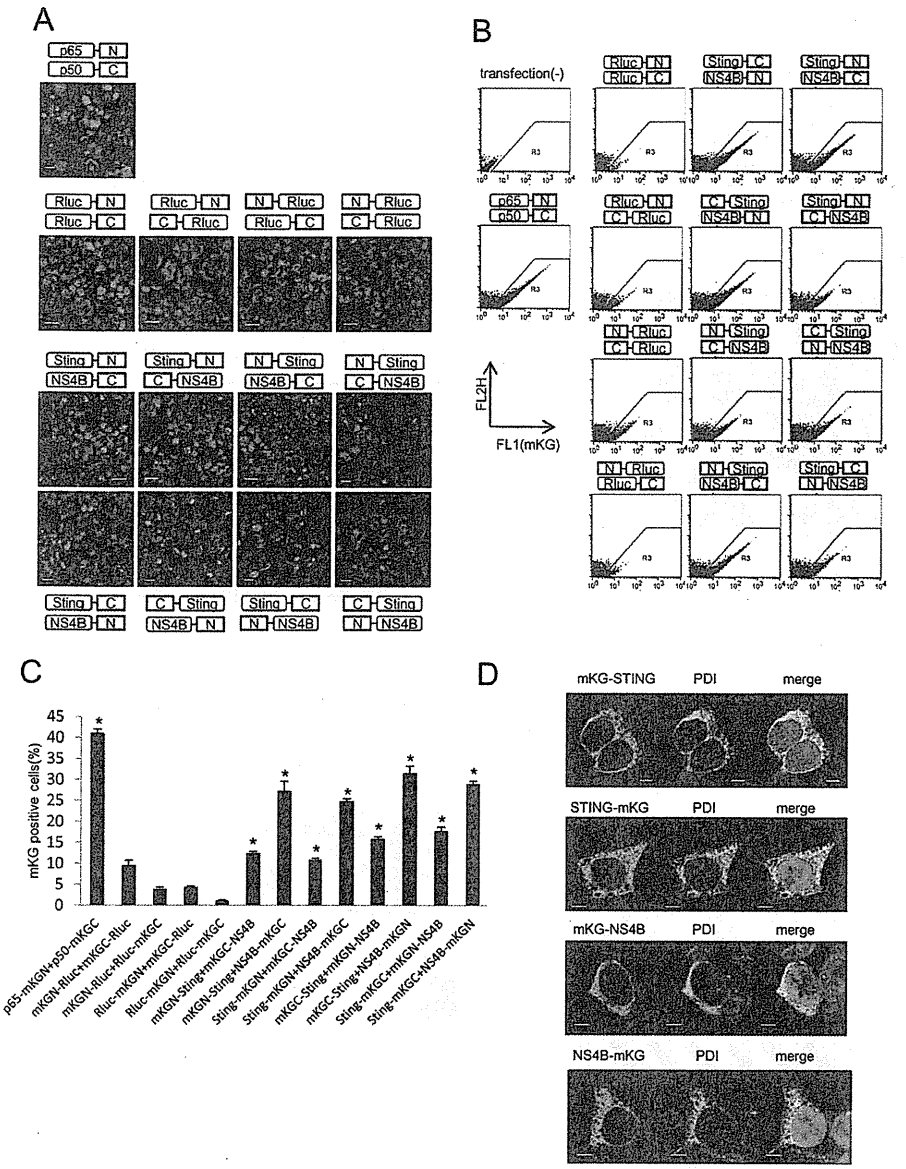

Fig. 3. BiFC assays of STING and NS4B. The complementary pairs of N- or C-terminally mKG-fused NS4B and STING expression plasmids were cotransfected in HEK293T cells. After 24 hours, the cells were fixed and observed by confocal microscopy (A) or subjected to flow cytometry to measure mKG-emitted fluorescence (BiFC signal) and to count BiFC signal-positive cells (B,C). Plasmids expressing p65-mKGN and p50-mKGC individually were used as a BiFC-positive control and plasmids expressing N- or C-terminally mKG fused Rluc were used as a negative control. The letters N and C denote complimentary N- and C-terminal fragments of mKG, respectively. Assays were performed in triplicate and error bars indicate the mean ± SD. Scale bars indicate 10 μm (A). *$P < 0.05$ compared with corresponding negative controls. (D) Plasmids expressing mKG fragment-fused STING or NS4B were transfected in HEK293T cells. After 24 hours, the cells were fixed and immunostained with anti-mKG and anti-PDI (ER) antibody. Nuclei were stained with DAPI. Cells were observed by confocal microscopy. Scale bars = 5 μm.

between NS4B, Cardif, and STING. To detect those interactions in living cells, we performed BiFC assays.[37,38] We constructed NS4B, Cardif, and STING expression plasmids that were N- or C-terminally fused with truncated mKG proteins, respectively. First, we cotransfected several different pairs of NS4B and STING expression plasmids that were fused with complementary pairs of N- or C-terminally truncated mKG. Strong fluorescence by mKG complexes (BiFC signal) was detected in all pairs of cotransfections, suggesting significant molecular interaction (Fig. 3A). In flow cytometry, all pairs of NS4B- and STING-mKG fusion proteins were positive for strong BiFC signal (Fig. 3B). The percentages of cells positive for BiFC signal were significantly higher in STING-mKG and NS4B-mKG fusion complexes than in corresponding controls (Fig. 3C). These results demonstrate that HCV-NS4B and STING proteins interact with each other strongly and specifically in cells. Fluorescence microscopy indicated that N- and C-terminal fusion of mKG onto NS4B and STING did not affect subcellular localization (Fig. 3D).

We next studied the molecular interaction between NS4B and Cardif by BiFC assay using NS4B and Cardif fusion plasmids that were tagged with complementary pairs of truncated mKG. Weak fluorescence was detected in cells transfected with the pairs N-Cardif and NS4B-C, N-Cardif and C-NS4B, C-Cardif and